БЪЛГАРСКА АКАДЕМИЯ НА НАУКИТЕ • BULGARIAN ACADEMY OF SCIENCES

ГЕОХИМИЯ, МИНЕРАЛОГИЯ И ПЕТРОЛОГИЯ • 40 • СОФИЯ • 2003
GEOCHEMISTRY, MINERALOGY AND PETROLOGY • 40 • SOFIA • 2003

Capitan-Dimitrievo pluton in Central Srednogorie, Bulgaria: Mineral chemistry, geochemistry and isotope evidence for magma-mixing origin

Borislav K. Kamenov, Albrecht von Quadt, Irena Peytcheva

Abstract. The Capitan-Dimitrievo pluton, intruded into the basement of the Rhodopian tectonic units near to the border area with Srednogorie zone, is situated in the southernmost end of the Etropole-Panagyurishte-Pazardjik magmatic and metallogenic strip. It represents a composite small body of Late Cretaceous age and is one of the examples of the barren plutons in the Central Srednogorie sector. Past ideas postulated a multi-stage crystallization inward of the body, result of normal fractional differentiation. The new field observations did not find sharp intrusive contacts between the intermediate rock varieties, which merge into one another. Mafic gabbro bands and enclaves are wide dispersed, bearing evidences of existence of magma-mingling and mixing processes. According to the revised petrographic nomenclature the dominant rocks are with transitional alkalinity – monzogabbro, monzodiorite, quartz-monzodiorite, monzonite and quartz-monzonite. Granodiorites are poorer presented. Various dykes cut the plutonic rocks. High-temperature foliation is found in the rocks as a sign for their syntectonic character. The mafic minerals are clinopyroxene, amphibole and biotite. The alkali feldspar is high orthoclase. Normal and reverse zonings and relics of some crystal grains and zones in disequilibrium with the host magmas are signs for an open-system evolution of the crystallizing magmas. Oscillatory and reverse zonings are typical for most of the plagioclase. The patchy sieve textured plagioclases in several crystal populations, with a complex history indicate rapid changes in crystallization environment, most likely due to convective transport between crystallizing boundary layer and the new pulses from the interior of the magma reservoir.

New whole-rock chemistry data, included trace-element geochemistry outlined two separate trends: high-K calc-alkaline and shoshonitic one. Harker's diagrams and the spidergrams confirm the two new-outlined trends. The chondrite-normalized *REE* patterns are in accord with an evolution from an enriched mantle source complicated by crust contamination. All geochemical features indicate a general destructive-plate environment and the transitional in alkalinity arc-related origin of the primary magmas. A complex interplay between crust-derived and mantle-originated parental magmas on the background of continuing crystallization differentiation is deduced.

The petrological and geochemical data are combined with precise U-Pb single grain zircon dating for the timing of the pluton. The intrusion age of 78.54 Ma is obtained for the prevailing quartz-monzodiorite variety of the pluton. Hf-isotope data of the zircons and Sr- and Nd-whole rock data provide additional information about the magma sources.

Many peculiarities of the geochemical and isotope variations are consistent with three-component magma-mingling and magma-mixing of magmas with contrasting compositions: basic mantle-derived, quartz-monzonitic evolved by crystallization or produced from deeper asthenospheric levels and granodioritic crust-originated. The Capitan-Dimitrievo pluton shows the similar isotope-geochemical characteristics with some of the composite plutons in the Central Srednogorie and its barren character is explained by the rapid uplift and deeper erosion than in the other ore-magmatic centers in the metallogenic zone

Key words: rock-forming mineralogy, geochemistry, isotopes, magma-mixing evolution.

Addresses: B. Kamenov – Sofia University, 1000 Sofia, Bulgaria; E-mail: kamenov@gea.uni-sofia.bg;
A. von Quadt – ETH-8092 Zűrich, Switzerland; I. Peytcheva – Central Laboratory of Mineralogy and Crystallography, 1113 Sofia, Bulgaria

Каменов, Б. К., А. фон Куадт, И. Пейчева 2003. Капитан-Димитриевският плутон в Централното Средногорие, България: минерално-химични, геохимични и изотопни данни, подкрепящи произход чрез смесване на магми. *Геохим., минерал. и петрол.*, **40**, 21-53.

Резюме. Капитан-Димитриевският плутон, внедрен във фундамента на Родопските тектонски единици близо до граничната зона със Средногорската зона, е разположен в най-южния край на магматичната и металогенна ивица Етрополе-Панагюрище-Пазарджик. Той е съставно малко тяло с къснокредна възраст и е един от примерите за безрудни плутони на субдукционния островнодъгов магматизъм в Централното Средногорие. По-старите възгледи обосноваваха, че сложният му състав е резултат на фракционнна кристализация и внедряване отвън навътре. Новите полеви наблюдения не откриват резки интрузивни контакти между промеждутъчните по състав скални разновидности, които прехождат плавно един в друг. Широко разпространени са мафични габрови ивици и включения, носещи доказателства за процеси на магмено размесване и смесване. Съгласно ревизираната петрографска номенклатура преобладаващите скали са с преходна алкалност – монцогабро, монцодиорит, кварцмонцодиорит, монцонит и кварцмонцонит. По-слабо представени са гранодиоритите. Разнообразни дайки секат плутоничните скали. Скалите са подложени на високотемпературна деформация, белег за синтектонския характер на плутона. Мафичните минерали са клинопироксен, амфибол и биотит. Алкалният фелдшпат е висок ортоклаз. Нормалната и обратна зоналност и реликтите от някои кристални зърна и зони в неравновесие с вместващата магма са признаци за еволюция на кристализиращите магми в отворена система. По-голямата част от плагиоклазовите индивиди са с типична осцилаторна и обратна зоналност. Петнесто-ситовидните плагиоклази в няколко кристални популации със сложна история на образуване, сочат за бързи промени в кристализационната среда, дължащо се най-вероятно на конвективен транспорт между кристализиращия граничен слой и новите импулси от вътрешността на магматичния резервоар. Новите анализи на скалите, в съчетание с геохимията на елементите-следи, очертават две серии: високо-калиево калциево-алкална и шошонитова, изразени и на Харкеровите диаграми и спайдерграмите. Моделите на разпределение на редките земи са в съгласие с еволюцията на един обогатен мантиен източник, усложнен от корово замърсяване. Всички геохимичните особености са характерни за една обстановка на деструктивна окрайнина и един преходен по алкалността островнодъгов произход на първичната магма. Изведено е сложно взаимодействие между корови и мантийни родоначални магми на фона на продължаващата кристализационна диференциация.

Петроложките и геохимични данни са съчетани с U-Pb данни за възраст от единични сепарирани цирконi. Получена е възраст от 78,7 Ma за преобладаващата кварцмонцодиоритова скална разновидност на плутона. Допълнителна информация за характера на магмените източници е получена от Hf-изотопни данни за цирконите и от Sr- и Nd-данни на общи скални проби.

Много от геохимичните и изотопни вариации се обясняват с три-компонентно размесване и смесване на магми с различаващи се състави: базична мантийна, кварцмонцонитова еволюирала чрез кристализация или произведена от по-дълбоки астеносферни нива и гранодиоритова корова. Капитан-Димитриевският плутон показва сходни изотопно-геохимични характеристики с някои от съставните плутони в Централното Средногорие. Неговата промишлена безрудност е обяснена с бързото издигане и по-дълбоката ерозия в сравнение с другите рудно-магматични центрове в металогенната зона.

Introduction

The Late Cretaceous magmatism in the Srednogorie zone of Bulgaria has been considered for a long time as the main metallogenic factor, bearing to formation of various ore deposits. Almost all major Cu-Au deposits of Bulgaria are emplaced within the confines of this zone and some of them are estimated as world-class type from the currently mined resources (Andrew, 1997). Among the many Late Cretaceous volcano-plutonic centres, exposed in the Central Srednogorie zone in Bulgaria, the Capitan-Dimitrievo pluton is the only one, which is not accompanied by economic ore mineralizations.

The Capitan-Dimitrievo pluton is located in the southernmost end of the transversal

deep-seated faulted magmatic and metallogenic strip Etropole – Panagyurishte – Pazardjik - Peshtera. Being one of the rare barren plutonic exposures of supposed Upper Cretaceous age, the pluton is not well studied petrologically. Its petrographic nomenclature is more or less known, but the magmatic evolution paths are not based on reliable data. Neither detailed mineralogical studies and contemporary geochemical analyses, nor isotope data are published for the rocks of the pluton. Previously the pluton was misunderstood (Boyadjiev, 1986) as a multi-stage body, crystallized inward in the sequence of rocks derived by several crystallization differentiation steps. The new field observations and specialized mapping did not find sharp intrusive contacts between the various intermediate rock varieties, which turned out to merge into one another. The extensive bulk-rock re-sampling accompanied by new wet silicate and trace-element analyses (2000-2003) gave rise to new idea of its origin. The aim of the present study is to demonstrate some lines of evidence supporting the idea of three-component mixing as well as to fill up the gaps in our knowledge and understanding of the magma evolution in the area. This first detailed mineralogical study will add more confidence to the origin of the pluton. In this paper we will combine the petrological and geochemical data with precise U-Pb single grain zircon dating from representative rocks of the pluton for the timing of the pluton. Hf-isotope data of the zircons and Sr-and Nd-whole rock data provide additional information about the sources of the magma.

Although the scanty porphyry copper mineralizations within the pluton are sub-economic today, it belongs to the Srednogorie metallogenic ore province, one of the most prospective in south-eastern Europe. We believe that the defining the temporal and chemical evolution of the igneous rocks of the pluton will contribute to the understanding of regional metallogenesis, associated with the Late Cretaceous geodynamic regime.

Geological background

The Capitan-Dimtrievo pluton, exposed between the villages Capitan-Dimitrievo, Radilovo and Byaga (Fig. 1) has a surface outcrop of around 18 km^2. It is emplaced into the Rhodopian basement metamorphic sequences near to the border area with the crystalline rocks of the Srednogorie zone. Recent exposures of the pluton represent a fragment of a bigger igneous body ~ 25 km^2 according to the drilling and geophysical studies (Dobrev et al., 1986). The preserved small graben-like block is covered to the north and east by Quaternary sedimentary deposits of the Upper Thracian Depression and to the south and west – by Paleogene sedimentary-volcanogenic sequences of the Peshtera graben (Dabovski, 1969). From northeast the marbles of the Rhodopian metamorphic sequences are overthrusted on the pluton. The west outline of the pluton meets another uplifted metamorphic block along a system of steep faults. Fragments of marbles are also overthrusted on this block. The country rocks are leptitoid gneisses and marbles. The contacts with the marbles are tectonic. Insignificant iron-ore mineralizations are known only north of the village Capitan-Dimitrievo and they should be genetically connected with the contact phenomena ([1]Kostov, 1947). The contact influence on the country rocks is clear expressed in the south-eastern flank of the pluton, where the Upper Cretaceous volcano-sedimentary complex (Boyadjiev, Ivanova-Panayotova, 1982) contains pyroxene hornfelses. The available several K-Ar radio-isotopic determinations on whole rock of quartz-monzodiorites and separated K-feldspar samples yielded ages in the span of 78.3-82.4 Ma (Boyadjiev, Lilov, 1981).

The movements along the Maritza strike-slip shear zone control the spatial position of

[1] Kostov, I. 1947. Iron-ore and copper-ore deposits in between the villages of Padalovo and Byaga, Peshtera district. - *Geofond Comm. Geol.*, 13-23.

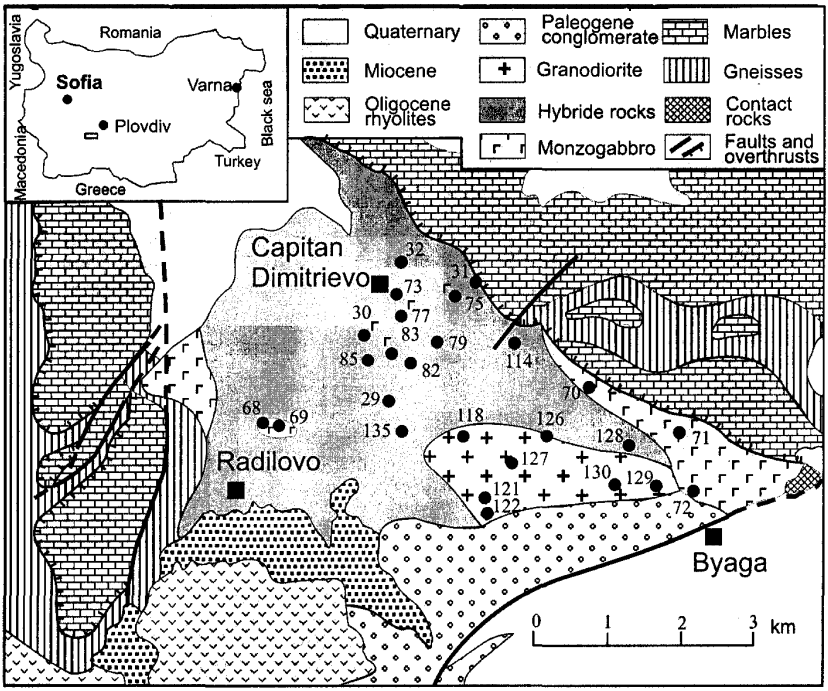

Fig. 1. Schematic geological map, based on new field revisions and the maps of Dabovski (1969) and Boyadjiev (1986). The black circles represent the sites of the new whole rock samples, analyzed for major oxides and trace elements

Фиг. 1. Схематична геоложка карта, съставена по нови полеви ревизии и картите на Dabovski (1969) and Boyadjiev (1986). Черните точки са местата на новите скални проби, анализирани за главни оксиди и елементи-следи

the pluton. The Late Alpine tectonic reworking of the plutonic rocks is strong, especially close to the contacts. A rather expressive high-temperature foliation is observed in the rocks. The predominant direction of S_1 is 10-50° dipping to the WNW at 55-88°. The foliation in individual sectors is directed 110-140° with dip to WS/30-70°. The elongated amphibole prisms show mineral lineation on some places (L_1=20°/35°). In the regional-tectonic or general geological papers the rocks of the pluton has been variably described as diorites, granosyenites and granites (Bonchev, 1938; Yaranov, 1940; [1]Katzkov, 1964), syenites and syenite-diorite (Dimitrov, 1939, 1946). Gabbro-diorites, diorites, granodiorites are the rock varieties mentioned by Kostov (1947) and [2]Boyanov (1957). According to Dabovski (1969) "contaminated" facies followed by quartzdioritic and quartz-monzodioritic ones are presented. The meso- and microstructural

[1] Katzkov, N. 1964. Report on the geology of the northern parts of Rhodopes between the town of Pashtera and the village of Krichim. *Geofond Comm. Geol.*

[2] Boyanov, I. 1957. Report on the geological mapping in scale 1:100 000 with reconnaissance works for the eastern part of the Western Rhodopes and partly the basin of Arda river, Bulgaria. *Geofond Comm. Geol.*

studies of Dabovski (1969) revealed the morphology of the magma-including structure of the pluton with a general direction of the long axis 150-160° and steep dip to the interior of the body.

The only paper devoted to the petrology and geochemistry of the pluton in more details is the one of Boyadjiev (1986). A wide range of rocks is described there – gabbro, diorites, quartz-monzodiorites, granodiorites, related through crystallization differentiation. The potential metallogeny of the pluton is defined by the content of Cu, Pb and Mo, determined above the Clark values. The past ideas (Dabovski, 1969; Boyadjiev, 1986) postulated that the pluton is multi-stage body crystallized inward.

Materials and methods

To obtain representative material for the magmatic history of the pluton 70 new fresh rock samples were collected. A total of 49 thin and 15 polished sections were examined by optical microscopy. Whole-rock major oxides were performed in the Chemical Laboratory of the Department of Petrology, Sofia University, by wet silicate analysis. Based on thin section studies, only 28 new silicate analyses and trace element data were obtained and they were used in a common set with additional 17 old and already published analyses for the interpretations. The localities of the samples are given in Fig. 1.

The chemical composition of the minerals was carried out using JEOL JSM 35 CF electron microprobe with Tracor Northern TN-2000 analysing system at the EUROTEST Co, Sofia. Operating conditions were 15 kV accelerating voltage with counting times of 100s and sample current of 2.10^{-9} A. Synthesized pure oxides and natural mineral standards were used. Oxide ZAF correction was applied to the analyses.

The trace and *REE* determinations are carried out using the laser ablation ICP-MS method. For further details we refer to Guenter et al. (2001).

High-precision "conventional" U-Pb analyses were carried out on single zircon grains at ETH, Zűrich. Measurements were made using an ion counter system (Finnigan MAT 262 thermal ionisation mass-spectrometer). For further details we refer to von Quadt et al. (2002). The PBDAT (Ludwig, 1988) and ISOPLOT programs of Ludwig (1991) were used for calculating the uncertainties, correlations of U/Pb ratios, and all errors are reported at the 2σ level. The decay constants of Steiger and Jäeger (1977) were used for age calculation, and corrections for common Pb were made using the values of Stacey and Kramers (1975).

Hf isotope ratios in zircon were measured in MC-ICPMS (David et al., 2001). For the calculation of the εHf values the following present-day ratios $(^{176}Hf/^{177}Hf)_{CH}$ 0.28286 and $(^{176}Lu/^{177}Hf)_{CH}$ 0.0334 are used, and for 79 Ma a $^{176}Lu/^{177}Hf$ ratio of 0.0050 for all zircons was taken into account.

The procedures for the whole rock isotopic analysis of Sm, Nd, Rb and Sr are modified from those reported by Richard et al. (1976) and further detailed by von Quadt (1997). Nd isotopic ratios were normalized to $^{146}Nd/^{144}Nd$ 0.7219. Analytical reproducibility was estimated by periodically measuring the La Jolla standard (Nd) as well as the NBS 987 (Sr).

Petrography and mineralogy

According to the new study the pluton consists of gabbro, monzogabbro, monzodiorite, quartz-monzodiorite, monzonite, quartz-monzonite and granodiorite (the modal nomenclature of Le Maitre et al., 1989). Not a single diorite specimen is found. The petrographical composition is variegated and changeable. These rock varieties can be incorporated into the following groups: basic rocks, hybrid group and evolved group. The contacts between these groups are more or less clear (Fig. 1). The basic group is composed of cumulates and gabbro. The rock varieties in this group are gradually passing over one into another. The

Table 1. *Chemical composition of selected plagioclases*
Таблица 1. *Химичен състав на избрани плагиоклази*

Rock	MGb	Md		QMd		Gd		Gd		Gb-p
Sample	71-a	73		72-a		127		130		84-b
Points	Pl_{17}-c	Pl_{44}-c	Pl_{45}-r	Pl_{69}-c	Pl_{70}-r	Pl_{86} -c	Pl_{87} -r	Pl_{66}-c	Pl_{65}-r	Pl_{61}-c
SiO_2	55.17	56.09	56.91	62.60	61.03	57.21	60.35	60.59	63.95	58.57
TiO_2	0	0.06	0.06	0	0	0	0	0	0	0
Al_2O_3	28.68	27.83	28.32	22.99	23.74	27.14	25.18	25.14	23.29	25.58
FeOt	0.35	0.34	0.14	0	0.24	0	0.14	0.21	0.17	0.25
MnO	0	0.09	0	0	0.12	0.19	0	0	0	0
MgO	0.48	0.64	0.30	0	0	0	0	0	0	0.16
CaO	9.47	8.47	8.49	8.50	9.53	8.31	6.49	6.07	3.85	10.98
Na_2O	5.43	6.20	5.36	5.65	4.91	6.77	7.78	7.72	8.51	4.15
K_2O	0.35	0.18	0.23	0.15	0.24	0.10	0.21	0.27	0.18	0.15
Total	99.93	99.84	99.81	99.89	99.81	99.72	100.15	100.00	99.95	99.80
An%	48.1	42.6	45.9	45.0	51.0	40.1	31.2	29.9	19.9	58.8
Ab%	49.8	56.4	52.6	54.1	47.5	59.2	67.6	68.5	79.0	40.2
Or%	2.1	1.0	1.5	0.9	1.6	0.7	1.2	1.6	1.1	1.0

Notes: MGb – monzogabbro, Md – monzodiorite, QMd – quartz-monzodiorite, Gd – granodiorite, Gb-p – gabbro porphyry dyke. c - core, r – rim
Забележки: MGb – монцогабро, Md – монцодиорит, QMd – кварцмонцодиорит, Gd – гранодиорит, Gb-p – габропорфиритна дайка. c - ядро, r – периферия

hybrid group of rocks is dominating in the area and it is the most varied (monzogabbro, monzodiorite, quartz-monzodiorite, monzonite and occasionally quartz-monzonite). The evolved group includes some extreme quartz-monzonites and granodiorites and occupies small area in the southern marginal part of the pluton. All transitional varieties between the gabbro, granodiorite and the extremely evolved quartz-monzonite can be traced in the outcrops.

The rocks have a medium-grained, essentially equigranular and rarely porphyrytic texture. Hypidiomorphic sequence of crystallization (monzonitic and granitic textures) is observed. The structure is massive to foliated close to the tectonic contacts. The major mineral is plagioclase. The mafic mineral assemblage is dominated by clinopyroxene, amphibole and biotite. Minor constituents are K-feldspar and quartz. Quartz amounts between 0-15 % in the hybrid rocks and between 18 and 21 % - in the granodiorite. Common accessory minerals include apatite, zircon, titanite, magnetite and ilmenite. Secondary minerals are epidote, tourmaline, chlorite, actinolite, adularia, calcite and clay minerals.

Colour index ranges 38-65 for the gabbro, 16-26 – for the hybrid intermediate varieties and 10-17 – for the granodiorites. The plutonic rocks are intruded by microgabbro and gabbro porphyry dykes with sharp and well-defined contacts. Rare quartz-monzodiorite porphyry and granodiorite porphyry dykes cut also the plutone. Pegmatites (including rare-metal microcline type tourmaline-bearing ones) and aplites are scarce. The wall-rock alterations are mainly K-silicate type, the propylitization being rarely presented. Hydrothermal quartz veins and disseminated pyrite and occasionally chalcopyrite are usually found in the rock, but the intensity of the alterations is weak on the today's erosional level.

Mafic microgranular and rounded enclaves occur often in all mesocratic rock varieties, some of them showing preserved chilled rims. They are composed of monzogabbro, melamonzodiorite or melaquartz-monzodiorite. The enclaves have a range in size from less than 1 cm to 30-40 cm and they are with sharp contacts with the host rock. Rough layering and cumulative packets of mafic minerals can be observed on some places. The ultramafic samples (pyroxene-amphibole cumulates) are

composed of almost monomineral pseudomorphs of hornblende after clinopyroxene.

Plagioclase composition (Table 1) spans almost all crystallization history of the pluton (An_{10}-An_{60}). A general consecutive decreasing of the average composition from gabbro to granodiorite samples is revealed. The average composition of the cores in the plagioclases from the gabbro is An_{48} (range An_{47}-An_{50}) and in the rims it is An_{50} (An_{49}-An_{51}). Monzogabbro shows slightly more acid plagioclases – average An_{38} (An_{36}-An_{41}) for the cores and An_{36} (An_{33}-An_{39}) for the rims. Normal and reverse zonings are present in the mafic rock varieties. Quartz-monzodiorite and monzodiorite contain plagioclases mainly within the range of andesine (average An_{49} at range of An_{43}-An_{57} for the cores and average An_{48} at range of An_{42}-An_{59} for their rims). Quartz-monzonite displays the average anorthite composition An_{18} (An_{14}-An_{25}) in the cores and An_{13} (An_{11}-An_{15}) in the rims. Plagioclases from the granodiorite vary in their anorthite composition in rather wide range. The average anorthite composition in this rock is An_{35} (An_{15}-An_{48}) for the cores and An_{25} (An_{14}-An_{42}) for the rims of the grains.

Plagioclase porphyries of the mafic dykes are with average An_{55} (An_{48}-An_{60}) in their cores and An_{52} (An_{50}-An_{53}) in their rims. Porphyry plagioclases of the quartz-monzodiorite-porphyry and granite-porphyry dykes are nearly within the same ranges – An_{40}-An_{45} average in the cores and An_{25}-An_{35} - - in the rims.

Oscillatory and patchy zonings are observed and the reverse pattern is typical for most of the plagioclases from the hybrid rocks. Complex normal zoning with inner cores overgrown by sharply more basic intermediate zones, measuring up to the gabbro anorthite levels (An_{55}) is sometimes their specific feature. Some of these peaks are in disequilibrium with the more evolved magmas. Sieve textured plagioclases, the several crystal populations with a complex history, saw-tooth zoning and smaller resorption zones indicate rapid changes in crystallization environment (Hibbard, 1981, 1991; Tsuchiama, 1985) most likely due to convective transport between crystallizing boundary layer and a new mafic pulse of the gabbro magma from the interior of the magma reservoir.

The availability of resorbed grains in wide range of anorthite compositions and of

Table 2. *Chemical composition of selected K-feldspars*
Таблица 2. Химичен състав на избрани калиеви фелдпати

Sample	31-I	BK/73	BK/30	BK/128			BK/130	BK/118	
Mineral	KF_9	KF_{13}	KF_{14}	KF_{15}	KF_{18}-c	KF_{19}-r	KF_{11}	KF_{26}-c	KF_{25}-r
Rock	MGb	Md	QMd	QMz			Gd		
SiO_2	62.90	62.25	62.60	63.12	63.04	62.29	66.25	64.94	64.63
Al_2O_3	19.15	20.23	20.55	20.68	20.73	20.30	15.66	18.03	18.29
FeOt	0	0.31	0	0	0	0.23	0.09	0	0.13
MnO	0	0	0	0	0	0.12	0	0	0
CaO	0	0	0	0.09	0.08	0	0	0.12	0.40
Na_2O	1.30	0.85	0.94	0.96	0.91	0.50	2.28	1.22	1.26
K_2O	15.69	15.63	15.55	14.45	13.90	16.17	14.77	15.28	14.51
BaO	0.42	0	0	0.58	0.41	0.15	0.74	0.57	0.28
Total	99.46	99.27	99.64	99.84	99.07	99.76	99.79	100.16	99.50
Or	88.1	92.4	91.6	89.4	89.8	95.2	80.1	87.7	86.0
Ab	11.1	7.6	8.4	9.0	8.9	4.5	18.7	10.7	11.5
An	0	0	0	0.5	0.4	0	0	0.6	2.0
Cn	0.8	0	0	1.1	0.9	0.3	1.2	1.0	0.5

Notes: The abbreviations are the same as in Table 1
Забележка: Съкращенията са същите, както в таблица 1

corroded cores, the observed several oscillations in the intermediate zones of the crystals from the hybrid rock varieties support also the wide-spread manifestations of magma-mingling and magma-mixing events during the crystallization of the plagioclases.

Potassium feldspar (0-25 vol.%) is orthoclase-microperthite having 80-95% Or (Table 2). Usually it occurs interstitially as a minor constituent in the monzogabbro (0-8 vol.%) and in the hybrid rocks (7-17 vol.%). Quartz-monzonite and granodiorite contain K-feldspar in the range 20-25% with larger size – up to 1.5-2.5 mm, sometimes porphyroid textures being typical. Overall, K-feldspar compositions in the more evolved rocks are richer in celzian component. Ba content of the K-feldspars decreases from their cores to the rims, in spite of the fact that in general feldspar large crystals are not apparently zoned, nor there are systematic directions of zoning for the other components. This suggests that the melt, from which they grew, was well-stirred during their growth or that the crystal growth rate was small compared to the diffusion rates in the remnant melt for K, Al, Na and Si.

Clinopyroxene represents the highest Mg/(Mg+Fe) phase among the constituent minerals. Its composition (Table 3) records a much more complex open-system evolution, in which the steady-state crystallization of the acid magma is linked to episodic injections of mafic magma into Capitan-Dimitrievo magma reservoir system. A rather small range of compositions in Ca-Fe-Mg space (Morimoto, 1988) is revealed. None of the rocks show consistent intracrystal patterns of zoning, except some grains from the gabbro, in which the rims are more calcic than the cores. Clinopyroxene is one of the principal mafic minerals in the gabbro and monzogabbro (10-20 vol.%), but it is a minor constituent (1-5 vol.%) in the intermediate hybrid rock varieties. Most of the clinopyroxene grains are replaced partly or entirely by late-magmatic amphibole. The intensity of this process increases to the more acid rock varieties. Quartz-monzodiorites contain only rare relics and normally the granodiorites are pyroxene-free. Two sets in size of the grains are observed. The smaller grains have average diameter of around 0.1-0.3 mm and the larger – 0.8-1.4 mm. The majority of the crystals record crystallization from a liquid comparable to the emplaced gabbro magma. They are auguites with average Mg# of 0.68-0.71 and their wollastonite constituent is 42-45% (Cr_2O_3 <

Table 3. *Chemical composition of selected clinopyroxenes*
Таблица 3. *Химичен състав на избрани клинопироксени*

Sample	BK/71-a				BK/30
Analysis	CPx_1 c	CPx_2 r	CPx_3 c	CPx_4 c	CPx_{12} m
Rock	MGb				QMd
SiO_2	50.09	50.90	50.91	51.01	50.52
TiO_2	0.26	0.13	0.13	0.15	0.12
Al_2O_3	3.81	3.77	3.73	4.04	3.03
FeO	10.11	10.05	9.44	10.21	8.17
MnO	0.87	0.60	0.72	0.92	0.77
MgO	12.58	12.89	13.56	13.35	12.85
CaO	21.77	20.99	21.02	19.95	23.60
Na_2O	0	0	0	0	0.85
K_2O	0	0.06	0.06	0	0
Total	99.49	99.39	99.57	99.63	99.91
Si	1.889	1.918	1.908	1.916	1.875
^{IV}Al	0.111	0.082	0.092	0.084	0.125
T	2.000	2.000	2.000	2.000	2.000
^{VI}Al	0.059	0.086	0.073	0.095	0.008
Ti	0.007	0.004	0.004	0.004	0.003
Fe^{3+}	0.037	0	0.014	0	0.171
Fe^{2+}	0.190	0.186	0.152	0.153	0.083
Mg	0.707	0.724	0.758	0.748	0.711
M1	1.000	1.000	1.001	1.000	0.976
Fe^{2+}	0.092	0.130	0.130	0.168	0
Mn	0.028	0.019	0.023	0.029	0.024
Ca	0.880	0.848	0.844	0.803	0.939
Na	0	0	0	0	0.061
K	0	0.003	0.003	0	0
M2	1.000	1.000	1.000	1.000	1.024
Wo	45.5	44.4	43.9	42.2	48.7
En	36.6	38.0	39.5	39.3	36.9
Fs	17.4	17.6	16.6	18.4	14.4
Mg #	0.672	0.683	0.704	0.681	0.719

Notes: Mg # = Mg/(Mg + Fe) (*apfu*); the other abbreviations are the same as in Table 1
Забележки: Mg # = Mg/(Mg+Fe) (*apfu*); другите съкращения са както в таблица 1

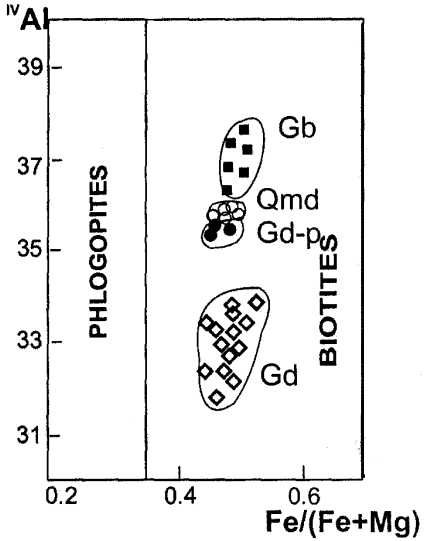

Fig. 2. Biotite composition in the plot ^{IV}Al vs. Fe/(Fe+ Mg)
Фиг. 2. Състав на биотити в диаграмата ^{IV}Al vs. Fe/(Fe+ Mg)

0.10 wt. %; Al/Ti 41-45). However, interesting is the findings of some small diopside grains from the monzogabbro and occasionally from the monzodiorite cored by low-Cr crystals, similar to the above described and rimmed by moderate-Cr rims (Cr_2O_3 0.10-0.20 wt. %; Mg# 72-75; wo_{46-49}; Al/Ti ~ 25). The presence of the last clinopyroxene grains suggests a complex open-system evolution of the crystallizing chamber. They might be a result of some input of more primitive mafic magma intro the base of a vigorously convecting chamber.

Biotite (2-10 vol.%) is less frequent in the gabbro and more often found in the hybrid varieties. Compositional variations (Table 4) in the averaged Mg# values for different rock varieties are narrow and all samples fall within the biotite of normal Al-bearing varieties. The Mg# average ratio ranges from 0.44 to 0.56, being 0.50 (range 0.49-0.52) in the gabbro, 0.53 (range 0.51-0.54) in the quartz-monzodiorite, 0.45 (range 0.44-0.50) in the quartz-monzonite and 0.52 (range 0.47-0.56) in the granodiorite. Granite-porphyry dykes contain biotite with Mg# in the range of 0.52-0.54. The evolution of biotite composition can be followed on the ^{IV}Al vs. Fe/(Fe+Mg) diagram in Fig. 2. The difference between the rocks varieties fields is due mainly to the divergence of the values of ^{IV}Al (*apfu*) of their biotites. The significant decreasing of these values from the gabbro to the granodiorite varieties is likely to be related with the depth of the biotite crystallization. The mixing of basic deeper-derived and acid shallower magmas is also in accord with the regular changes in these compositional features. Biotites from the porphyry dykes and hybrid rock varieties are located between the mafic and felsic mixing magma components.

The MgO vs. Al_2O_3 (wt. %) diagram of Abdel-Rahman (1994) provides discrimination for the biotites from the pluton (Fig. 3). All samples fall in the field of the calc-alkaline rocks. The general trend showing a gradual increase in MgO with decreasing Al_2O_3 is remarkable for the biotites studied. It suggests the following substitution between Mg and Al in octahedral sites: $3Mg \rightarrow 2Al$.

Amphibole. All amphiboles analysed in our data set (Table 5) are calcic amphiboles, according to the terminology of Leake et al., (1997). They are characteristic constituents of

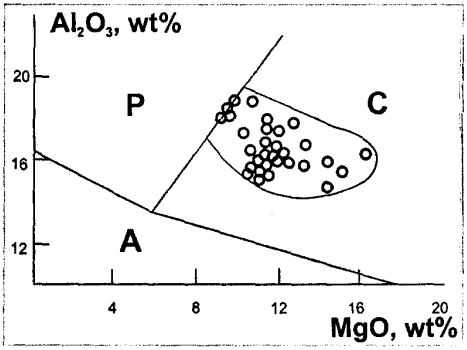

Fig. 3. MgO vs. Al_2O_3 (wt. %) discrimination diagram after Abdel-Rahman (1994). Settings: A – alkaline, P – peraluminous, C – calc-alkaline
Фиг. 3. MgO vs. Al_2O_3 (тегл. %) по Abdel-Rahman (1994). Обстановки: A – алкална, P – свръх-алуминиева, C – калциево-алкална

Table 4. *Chemical composition of selected biotites*
Таблица 4. *Химичен състав на избрани биотити*

Sample	BK/71-a		BK/30	BK/128		BK/130	BK/127	BK/32	
Analysis	Bt_{48}-c	Bt_{49}-r	Bt_{143}-c	Bt_{15}-c	Bt_{19}-c	Bt_{10}-c	Bt_{24}-c	Bt_{124}-c	Bt_{125}-c
Rock	MGb		QMd	QMz		Gd		Gd-p	
SiO_2	35.24	34.04	35.59	36.06	35.07	38.00	37.09	36.05	36.02
TiO_2	2.48	2.32	3.10	2.02	1.69	1.62	2.35	1.94	1.54
Al_2O_3	16.33	16.83	16.76	18.00	18.35	16.22	15.64	17.57	17.73
FeOt	20.29	21.77	18.80	19.42	20.68	18.83	19.02	18.47	18.00
MnO	0.29	0.34	0.59	0.28	0.24	0.30	0.51	0.60	0.62
MgO	12.06	11.65	11.19	10.66	9.54	11.35	10.95	11.15	11.34
CaO	0	0.07	0	0	0	0	0	0	0
K_2O	9.43	8.85	9.69	10.10	10.38	10.27	10.49	10.16	10.03
Total	96.12	95.87	96.16	96.54	95.95	96.12	96.05	95.94	95.28
Si	5.129	5.002	5.165	5.194	5.133	5.444	5.382	5.216	5.231
^{IV}Al	2.799	2.912	2.835	2.806	2.867	2.556	2.618	2.784	2.769
^{IV}Ti	0.072	0.086	0	0	0	0	0	0	0
^{VI}Al	0	0	0.030	0.247	0.296	0.180	0.055	0.210	0.264
^{VI}Ti	0.199	0.170	0.338	0.219	0.186	0.175	0.256	0.211	0.168
Fe^{2+}	2.470	2.675	2.282	2.339	2.531	2.256	2.308	2.235	2.186
Mn	0.036	0.042	0.073	0.034	0.030	0.036	0.063	0.074	0.076
Mg	2.617	2.552	2.421	2.289	2.082	2.424	2.369	2.405	2.455
Y	5.322	5.439	5.144	5.128	5.125	5.071	5.051	5.135	5.149
Ca	0	0.011	0	0	0	0	0	0	0
K	1.750	1.659	1.833	1.856	1.938	1.877	1.942	1.875	1.858
X	1.750	1.670	1.833	1.856	1.938	1.877	1.942	1.875	1.858
Mg #	0.514	0.488	0.515	0.495	0.451	0.518	0.506	0.518	0.529

Notes: All abbreviations as in Table 1
Забележка: Всички съкращения са както в таблица 1

all rock varieties of the pluton. The modal percentage of amphibole in the gabbro ranges 20-40, in the hybrid rocks – 13-22 and in the granodiorite 5-10. Adopting the IMA-nomenclature the cation ratio $X_{Mg} = Mg/(Mg+Fe^{2+})$, the Si-content and the A-site occupancy $(Na+K)_A$ enable the amphibole compositions to be illustrated in Fig. 4a-c. In spite of some overlapping of the ranges for individual rock varieties, certain important features are worthy to be noted. Most of amphibole compositions from the gabbro are magnesiohornblende and tschermakite (Fig. 4b). The hybrid rocks (monzogabbro, monzodiorite, quartz-monzodiorite) contain more often tschermakites and magnesiohastingsites. The amphiboles of the granodiorite are richer in alkalies – edenites and magnesiohastingsite predominate in the rocks. Quartz-monzonite has only magnesiohastingsite as rock-forming mineral.

The ^{IV}Al vs. $(Na+K)_A$ plot (Fig. 4c) displays two trends. The first one confines the amphiboles of all rock varieties without the ones from the granodiorite. The elongation of this trend is easily explained with the substitution $3^{IV}Al \leftrightarrow 1A$ site, which is characteristic for some combination between tschermakite and edenite type of exchange. The mixing of quartz-monzonitic end member with its typical magnesiohastingsite amphibole with gabbro member (tschermakite and magnesiohornblende) might explain the hybrid rocks bearing in their amphiboles all possible combinations between these two mixing components. In fact, this amphibole trend corresponds to the shoshonitic trend in the rocks. The granodioritic trend of their amphibole composition is in sharp contrast to

Table 5. *Chemical composition of selected amphiboles*
Таблица 5. *Химичен състав на избрани амфиболи*

Rock	Gabbro		Monzogabbro		Quartz-monzodiorite		Granodiorite		Micro-diorite
Sample	BK/71-a		BK/31-I		BK/30		BK/118		84-b
Analysis	Hb_{15}-c	Hb_{71}-c	Hb_{16}-c	Hb_{17}-r	Hb_{42}-c	Hb_{44}-r	Hb_{51}-c	Hb_{52}-r	Hb_{62}
SiO_2	43.94	43.95	43.17	43.67	45.18	42.25	44.98	44.36	43.05
TiO_2	0.85	0.90	1.21	1.26	0.86	0.71	1.00	0.77	1.11
Al_2O_3	10.33	10.84	10.25	10.57	9.14	11.22	9.60	10.29	12.46
FeO_t	17.18	16.37	17.73	16.54	17.25	17.23	16.10	17.45	17.23
MnO	0.60	0.78	0.67	0.73	0.56	0.57	0.69	0.73	0.62
MgO	11.34	10.62	10.43	10.88	11.43	11.62	10.29	8.99	9.53
CaO	11.90	11.53	12.10	11.56	10.61	11.44	11.78	12.12	11.51
Na_2O	1.02	1.32	0.92	1.26	1.93	1.76	2.29	2.22	1.10
K_2O	0.90	1.28	1.54	1.47	0.85	1.04	1.23	1.16	1.34
Total	98.06	97.59	98.02	97.94	97.81	97.84	97.96	98.09	97.95
	Structural formulae based on 13 cations								
Si	6.453	6.523	6.433	6.470	6.634	6.226	6.776	6.731	6.381
^{IV}Al	1.547	1.477	1.557	1.530	1.366	1.774	1.234	1.269	1.619
^{VI}Al	0.239	0.420	0.247	0.316	0.216	0.175	0.466	0.570	0.558
Ti	0.094	0.100	0.136	0.140	0.095	0.079	0.113	0.088	0.124
Fe^{3+}	0.917	0.566	0.609	0.839	0.913	1.131	-	-	0.589
Fe^{2+}	1.193	1.466	1.604	1.211	1.205	0.992	2.025	2.214	1.547
Mg	2.483	2.349	2.320	2.402	2.501	2.552	2.307	2.034	2.105
Mn	0.074	0.098	0.084	0.092	0.070	0.071	0.088	0.094	0.078
Ca	1.872	1.834	1.935	1.727	1.669	1.806	1.898	1.970	1.828
Na-M4	0.128	0.166	0.065	0.273	0.331	0.194	0.102	0.030	0.172
Na-A	0.163	0.214	0.201	0.089	0.219	0.309	0.566	0.624	0.256
K	0.169	0.242	0.293	0.278	0.159	0.196	0.236	0.225	0.214
ΣA	0.332	0.456	0.494	0.367	0.378	0.505	0.802	0.849	0.470
Mg #	0.675	0.616	0.591	0.665	0.675	0.720	0.533	0.479	0.541
$Fe^{3+}/Fe^{2+}+Fe^{3+}$	0.434	0.278	0.275	0.409	0.431	0.533	-	-	0.169
Type	Tsc	MHb	Tsc	Tsc	MHb	MHas	Ed	FEd	Tch

Notes: 1. c – core, r – rim. 2. Nomenclature after Leake et al. (1997): Tsc – tschermakite; MHb – magnesiohornblende; MHas – magnesiohastingsite; Ed – edenite; Fed – ferro-edenite. 3. Mg # = Mg/(Mg + Fe^{2+}) (*apfu*). 4. The crystallo-chemical formulae are calculated on the basis of 13 cations FM=13 *apfu*, after Anderson, Smith (1995) and Fe^{2+} and Fe^{3+} are relocated according to Spear, Kimball (1984)
Забележки: 1. c - ядро, r - периферия. 2. Номенклатура по Leake et al. (1997): Tsc – чермакит; MHb – магнезиев обикновен амфибол; MHs – магнезиохейстингсит; Ed – еденит; Fed – фероеденит. 3. Mg # = Mg/(Mg + Fe^{2+}) (*apfu*). 4. Кристалохимичните формули са изчислени на основата на 13 катиона FM=13 (*apfu*) по Anderson, Smith (1995), а Fe^{2+} и Fe^{3+} са разпределени по Spear, Kimball (1984)

the first one. The later trend visualises the HK-CA trend in their rocks, result of mixing between a crust-derived acid magma and the mantle-derived gabbro magma. The edenites and the magnesiohastingsites are then a result of such mixing and that is why the edenite exchage is more typical for them.

Normal and reverse zonings are observed in the amphibole compositions, the last ones prevailing. Reverse moderate zoning is typical in amphiboles from the hybrid rock varieties (monzogabbro, monzodiorite and quartz-monzodiorite), whereas a normal one is a feature of the amphiboles from the gabbro. The

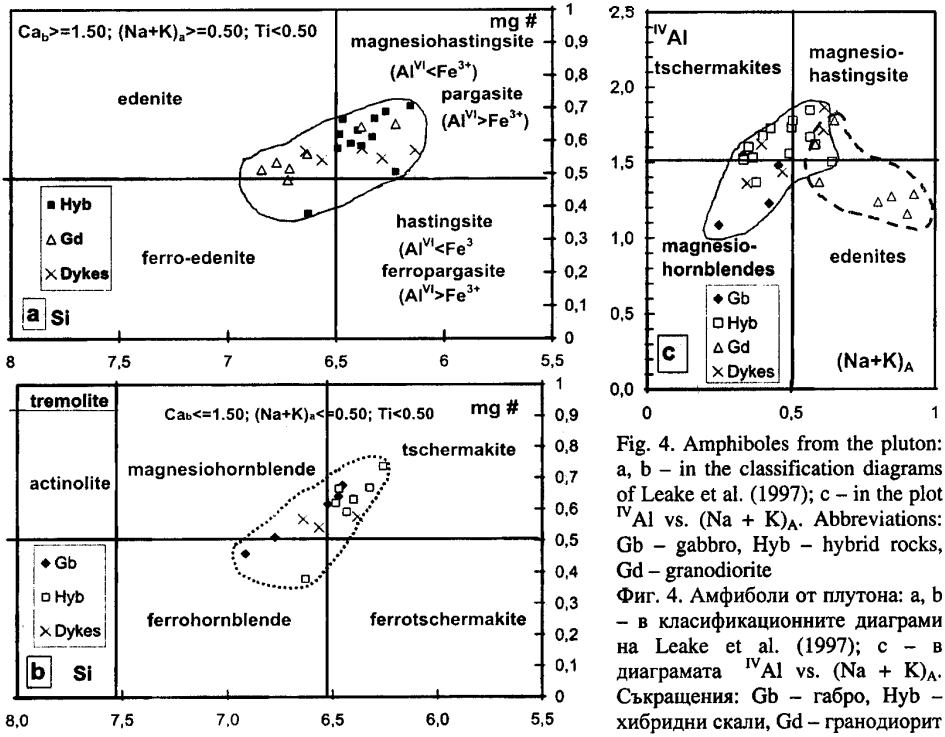

Fig. 4. Amphiboles from the pluton: a, b – in the classification diagrams of Leake et al. (1997); c – in the plot ^{IV}Al vs. $(Na + K)_A$. Abbreviations: Gb – gabbro, Hyb – hybrid rocks, Gd – granodiorite

Фиг. 4. Амфиболи от плутона: a, b – в класификационните диаграми на Leake et al. (1997); c – в диаграмата ^{IV}Al vs. $(Na + K)_A$. Съкращения: Gb – габро, Hyb – хибридни скали, Gd – гранодиорит

ratio Mg# in the amphiboles from the later rock diminishes slightly from the cores (0.64 at range of 0.61-0.68) to the rims (0.61 at range of 0.51-0.63). Amphiboles from the monzogabbro have average Mg# ratio of 0.66 (range 0,59-0.74) for their cores and 0.64 (range 0.58-0.67) – for their rims. Both types of zonings are characteristic for them. Amphiboles from monzodiorite and quartz-monzodiorite are typical for their reverse zoning. The ratio Mg# ranges in these amphiboles from 0.64 to 0.68, average 0.66 (core) to 0.70-0.75, average 0.72 (rim). The relationship between end members of the magmatic amphiboles depends primarily on the thermodynamic crystallization conditions and also on the degree of magma evolution progress (Wones, 1981). The ratio Mg# is usually correlated with the temperature of crystallization. The reverse zoning found in most of the amphiboles from the hybrid rock varieties should be explained as a mineralogical trace of an input of more primitive mafic magma into the crystallizing acid magma chamber.

Amphiboles from the granodioritic end member of the magma-mixing process are lower-temperature product of the crystallization of the acid magma, judging by their ratios Mg# - average 0.52 (range 0.51-0.54) for the cores and 0.50 (range 0.48-0.52) for the rims. The only representative of the mafic dykes analyzed has amphiboles with average ratio Mg# of 0.56 (core of the phenocrystals).

The clear correlation between the ratio Mg# and Si (Fig. 4c), Al, Ti, and alkalies is not disturbed in the rims of the amphiboles analyzed, so the sub-solidus fluid reworking of the rocks was weak and did not influence the amphibole compositions. Probably this conclusion has something to do with the lack of economical ore mineralizations related to the pluton.

The tetrahedral aluminium ^{IV}Al (*apfu*) in the amphiboles generally decreases with the differentiation of their magmas and with decreasing of temperature, at constant pressure, aH_2O, fO_2, and bulk composition. These contents are perceived also as an indicator of the crystallization pressure (Thomas, Ernst, 1990), but could depend on the activity of Si and on the degree of polymerization of the magma. The average ^{IV}Al (*apfu*) of the amphiboles from the gabbro is 0.480. The same parameter for the amphiboles from the monzogabbro is much lower – 0.248. For the amphiboles from the hybrid monzodiorites and quartz-monzodiorites it is 0.182. This tendency is disturbed in the granodiorites, where ^{IV}Al of their amphiboles is average 0.500 and in the gabbro-porphyry dykes it is average 0.520. Since the total Al (*apfu*) of amphiboles from the gabbro and for the hybrid varieties is more or less similar, and usually it is directly related with the crystallization pressure (Anderson, Smith, 1995), we speculate that different degrees of polymerization of the magmas are responsible for the formation of this tendency. An increasing of PH_2O in the sequence gabbro-hybrid magmas is in line with such assumption.

The higher ^{VI}Al (*apfu*) in the amphiboles of the dykes is probably related to their a bit deeper level of crystallization. Probably, the granodiorites with their rather high ^{VI}Al (*apfu*) in the amphiboles, have crystallized from magma with higher degree of polymerization and poorer in H_2O.

The zoning in amphiboles is accentuated by tracing of the abundances of Si (*apfu*). Average Si in the cores is lower than in the rims. The quite wide range of Si in the span of 6.30-6.90 proves the availability of different mixing proportions in the chamber of crystallization.

Calculated $Fe^{3+}/(Fe^{2+} + Fe^{3+})$ ratio in the amphiboles, based on 13 cations and charge balance shows that an increase of the oxidizing conditions from the gabbro to the hybrid magmas is recorded in these ratios. The average ratio in the amphiboles from the gabbro is 0.35 (range 0.21-0.40) and in the ones from the hybrid rocks – 0.50 (range 0.35-0.54).

Fe-Ti oxides. Analyses of Fe-Ti oxides are shown in Table 6. The oxide grains are fairly homogeneous, but some small compositional differences exist between different grains. *Magnetite* is an Al-poor (Al_2O_3 < 0.40 wt. %), Ti-poor (< 0.70 wt. %, therefore ulvospinel end-member is bellow 2%), Mn-, Cr-, and V-poor variety (V_2O_3 < 1 wt. %) variety. *Ilmenite* is a pyrophanite-moderate (0.1-0.2 mole fraction) and hematite-poor (0.01-0.10 mole fraction) phase, usually exsolved in lamellae. Manganese contents in the ilmenite are between 5 and 8 wt. %.

Geochemistry

The new and selected published whole-rock silicate analyses (Table 7) plotted on the diagram ($Na_2O + K_2O$) vs. SiO_2 (Bogatikov et al., 1981) are demonstrated in Fig. 5 a. Hybrid varieties classified by their modal relationship form a heavily populated field, localized between the fields of the gabbro and the granodiorite. Most of the samples fall in the row of the transitional in alkalinity suites and only the small number of the monzodiorites, quartz-monzodiorite and the majority of the granodiorites are displayed bellow the dividing line. It seems that either normal fractionation, or simple magma mixing could explain these peculiarities. The large variations in SiO_2 range and the low $Al_2O_3/(Na_2O + K_2O + CaO)$ ratio (< 1.1 mole proportions) together with the presence of magnetite, titanite and apatite inclusions in the biotite are evidence for I-type characteristics. All rocks are metaluminous and comprise varieties from slightly Si-undersaturated up to slightly Si-oversaturated. Peackok's index is around 56 referring to the transitional in alkalinity suites.

Two serial trends are revealed in the pluton on the K_2O vs. SiO_2 diagram (Fig. 5b after Peccerillo, Taylor, 1976, with the additions by Dabovski et al., 1989) for the first time: high-K calc-alkaline and shoshonitic one.

Table 6. *Chemical composition of selected Fe-Ti oxide minerals*
Таблица 6. *Химичен състав на избрани Fe-Ti оксидни минерали*

Type	Primary Ti-Fe oxides					
Sample	BK/71-a				BK/73	
Mineral	Ilm_1	Ilm_5	Mt_2	Mt_3	Mt_4	Mt_5
Rock	MGb				Md	
SiO_2	0.27	0.29	0.44	0.31	0.49	0.82
TiO_2	47.43	51.13	0	0.26	0.43	0.64
Al_2O_3	0.37	0	0	0	0	0.33
Fe_2O_3	9.09	1.08	67.26	66.48	66.48	64.71
FeO	37.44	37.54	31.62	31.20	32.76	32.52
MnO	5.46	8.57	0	0.11	0.13	0
MgO	0	0	0	0	0	0
CaO	0	0.08	0	0	0	0.09
K_2O	0	0	0	0	0	0
V_2O_3	0.55	0.43	0.89	0.54	0.69	0.48
Total	100.6	99.12	100.21	98.90	101.75	99.59
Si	0.007	0.07	0.017	0.012	0.018	0.032
Ti	0.896	0.978	0	0.008	0.012	0.018
Al	0.011	0	0	0	0	0.015
Fe^{3+}	0.172	0.021	1.947	1.949	1.925	1.875
Fe^{2+}	0.787	0.798	1.017	1.016	1.027	1.047
Mn	0.116	0.185	0	0.004	0.004	0
Mg	0	0	0	0	0	0
Ca	0	0.002	0	0	0	0.004
K	0	0	0	0	0	0
V	0.011	0.009	0.018	0.011	0.014	0.010
Cations	2.000	2.000	2.999	3.000	3.000	3.001
Ilm	79.6	80.4	-	-	-	-
Phyr	11.7	18.6	-	-	-	-
Hem	8.7	1.0	-	-	-	-
Ulv	-	-	-	0.8	1.2	1.9

Notes: Ilm- ilmenite, Mt – magnetite, Phyr – phyrophanite, Hem – hematite, Ulv – ulvospinel; the other abbreviations are as in Table 1
Забележки: Ilm - илменит, Mt - магнетит, Phyr - пирофанит, Hem - хематит, Ulv – улвошпинел, другите съкращения са както в таблица 1

The first one includes the samples of the gabbro, monzodiorite, quartz-monzodiorite and granodiorite, arranged in one mixing line. The second one includes samples of the gabbro, monzogabbro, monzonite and quartz-monzonite arranged in other line of mixing or fractional crystallization. The ratios Y/Zr, Zr/Hf and TiO_2/Zr imply fractionation of Ti due to clinopyroxene and oxide phases separated from the magma. A combination of the Ol-CPx-Hb ± Mt as fractionating phases is indicated by these geochemical data. This fractionation had been realized probably concurrently with the magma-mingling and magma-mixing events.

In the Harker diagrams (Fig. 6) the evolution seems continuous from the gabbro to the granodiorite at first sight, since there is no compositional gap for some of the oxides (CaO vs. SiO_2; TiO_2 vs. SiO_2 – not shown ect.).

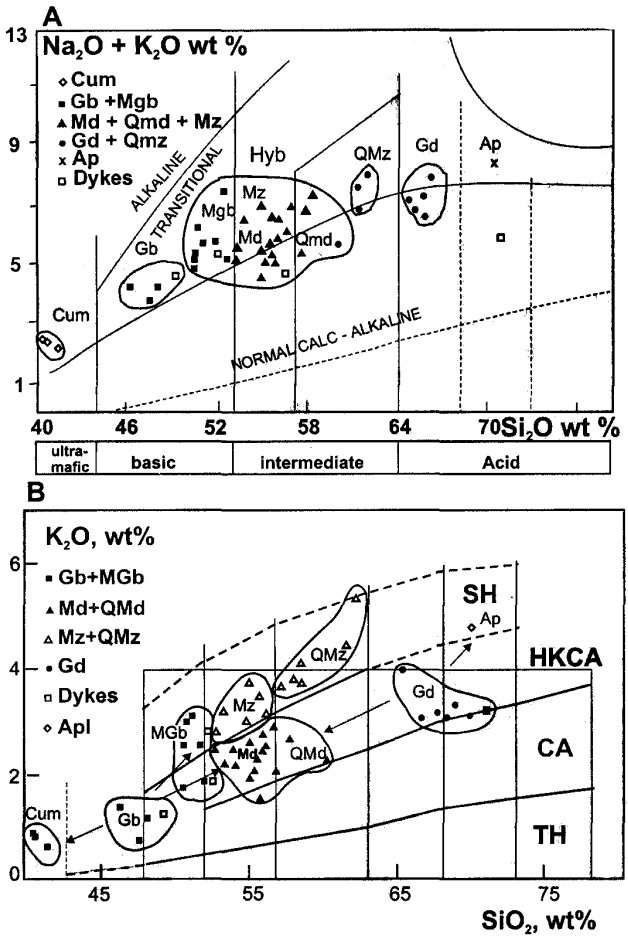

Fig. 5a. Plutonic rocks from the Capitan-Dimitrievo pluton in the plot SiO_2 vs. ($Na_2O + K_2O$) after Bogatikov et al. (1981). The rock names are after the nomenclature by Le Maitre (1989). Abbreviations: Cum – cumulative gabbro, Gb – gabbro, MGb – monzogabbro, Md – monzodiorite, Mz – monzonite, QMd – quartz-monzodiorite, QMz – quartz-monzonite, Gd – granodiorite, Ap – aplite and Hyb – hybrid varieties; b. Serial trends in Capitan-Dimitrievo pluton in the K_2O vs. SiO_2 plot (Peccerillo, Taylor, 1976) expanded (dashed lines) by Dabovski et al. (1989). Series: TH – tholeiitic; CA – calc-alkaline; HKCA – high-potassium calc-alkaline; SH – shoshonitic

Фиг. 5a. Плутоничните скали от Капитан-Димитриевския плутон в диаграмата SiO_2 vs. ($Na_2O + K_2O$) по Bogatikov et al. (1981). Скалните наименования са по номенклатурата на Le Maitre (1989). Съкращения: Cum - кумулативно габро, Gb - габро, MGb - монцогабро, Md - монцодиорит, Mz - монцонит, QMd - кварц-монцодиорит, QMz - кварц-монцонит, Gd - гранодиорит, Ap - аплит, Hyb - хибридни разновидности; b. Сериални трендове в Капитан-Димитриевския плутон в диаграмата K_2O vs. SiO_2 (Peccerillo, Taylor, 1976) разширена (щрихираните линии) от Dabovski et al. (1989). Серии: TH - толеитова, CA- калциево-алкална, HKCA - високо-калиево калциево-алкална, SH - шошонитова

Some of the oxides and elements are correlated also with SiO_2, but with a great deal of scattering. The steeper slopes for some oxides in the quartz-monzonite and some monzonites (e.g. MgO, CaO, FeO_T, Al_2O_3) may indicate a change in the crystallizing assemblage. However, the possible fractionation relation between the revealed two trends is not supported by the small compositional overlap obvious between the granodiorite and the other rocks. The trend connecting the end-samples of quartz-monzonite and the gabbro is characterized with greater fractionation of the mafic minerals and the involving of the plagioclase in the fractionating assemblage quite late in the sequence of crystallization. Conversely, the revealed different trends in the Harker plots rule out such an evolutionary link, i.e. the one trend could not be derived from the other. The two trends in the Harker diagrams are another expression of the magma-mixing relations between the three above-stated magma components. Most of the trace elements (Table 7) plotted against SiO_2 confirm the availability of the both evolution lines. On the plots of Zr, Hf, Pb, Co (Fig. 6) vs. SiO_2 the two trends appear clearly. They are expressed also on the plots of Rb/Sr, Th/Yb, Th/Hf, Y/P_2O_5, Y/Nb, TiO_2/Zr and many other ratios against SiO_2 (Fig. 7). The ratio Rb/Sr clearly increases with differentiation progress.

The ratios La/Sm vs. SiO_2 and La/Yb vs. SiO_2 (Fig. 7c,d) show again the two magma-evolution trends. The shoshonitic trend reveals steeper trend in the both plots in comparison with the high-K-calc-alkaline trend. At the value of the Peackok's index of 56 % SiO_2 the shoshonitic trend has ratio La/Sm close to 6 while in the high-K calc-alkaline trend it is around 4.5. The ratio La/Yb is even more indicative for these differences. At the same Peackok's index this ratio is close to 30 in the first trend and around 13 in the second one. The progressive increase of the *LREE* enrichments is a consequence of both different sources and process variation. The stronger increase of these *REE* ratios in the first trend is indicative not only for the source characteristics of the end-magma components, but also for the influence of the fractionation, amplifying the increase of the *REE*-enrichment.

Chondrite-normalized *REE* patterns (Fig. 8a-d) display regular variations only if the samples are arranged in the following sets: (a) gabbro-monzogabbro; (b) gabbro-monzogabbro-monzonite-quartz-monzonite; (c) gabbro-monzodiorite-granodiorite; (d) dykes. The *REE* enrichment relative to chondrite is quite large (La_N=60-1200, but normally to 210). The degree of enrichment of the *LREE* relative to *HREE* measured by the ratio $(La/Lu)_N$ is 5.3-6.6 in the gabbro, 7.9-8.5 in the monzogabbro (Fig. 8a) and 7.1-63.7 - in the quartz-monzonite (Fig. 8b).

The variations in the gabbro set and in the shoshonitic trend are due mainly to the left side of the plots – the ratio $(La/Sm)_N$ = 1.7-1.9 in the gabbro, 2.6-2.8 in the monzogabbro and 2.7-5.3 in the quartz-monzonite. *ΣREE* ranges between 128 –195 ppm in the gabbro, 188-245 ppm in the monzogabbro and 216-1570 ppm in the quartz-monzonite. The heavy *REE*-side of the patterns is almost flat. Europium anomaly is not detected in the more-primitive gabbro, monzogabbro and monzonites, but it is quite deep and expressive in the quartz-monzonite. This feature contradicts to the previous idea (Boyadjiev, 1986) that the normal crystallization differentiation is the only magma evolution process. The differences in the model of the *REE* distributions manifest a likely combination of the magma-mixing process between the gabbro end-member and the quartz-monzonite one (which is in sharp discrepancy with the other samples in the trend) and the continuing fractionation crystallization. This extreme magma end-composition could be derived in the same magma chamber from the fractionation of the parental basic magma, when the plagioclase had been included in the fractionating mineral association (the deep negative Eu-anomaly is

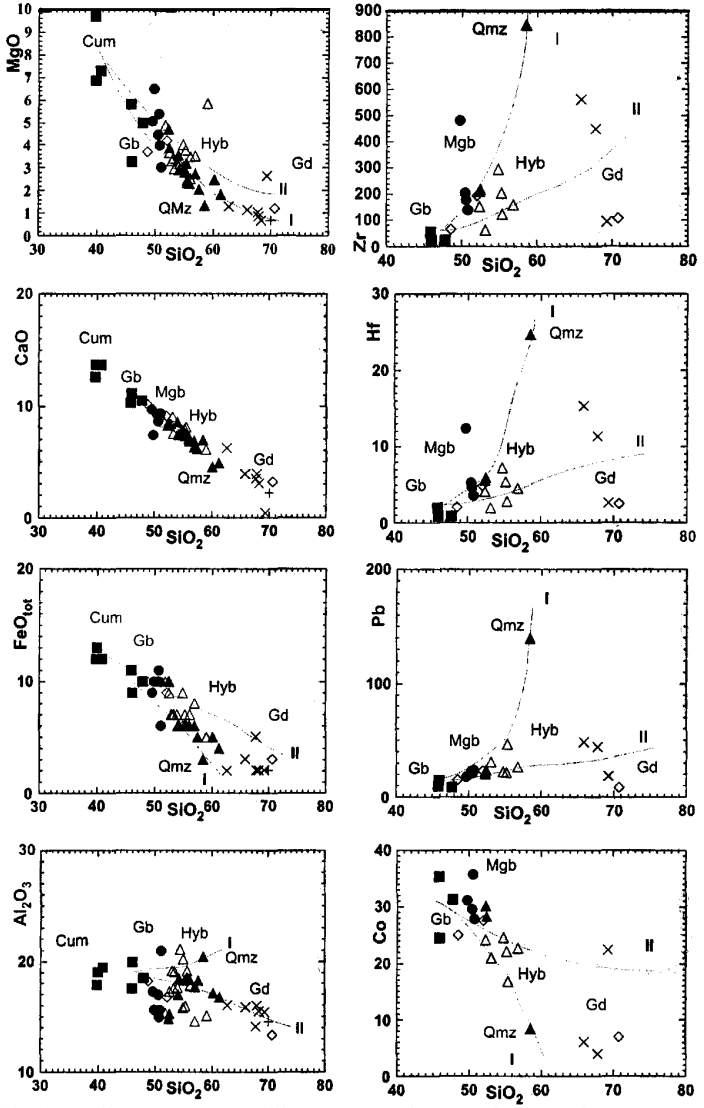

Fig. 6. Selected Harker's diagrams (major oxides and trace elements) for rocks from the Capitan-Dimitrievo pluton. The abbreviations are as in Fig. 5. Symboles: filled squares – gabbro; filled circles – monzogabbro; filled triangles – quartz-monzodiorites, monzonites and quartz-monzonites; empty triangles – monzodiorites; crosses – granodiorites; diamonds – dykes. Trends: I – shoshonitic, II – high-K calc-alkaline

Фиг. 6. Избрани харкерови диаграми (главни оксиди и елементи-следи) за скали от Капитан-Димитриевския плутон. Съкращенията са както на фиг. 5. Символи: плътни квадратчета – габро; плътни кръгчета – монцогабро; запълнени триъгълници – кварц-монцодиорити, монцонити и кварц-монцонити; кухи триъгълници – монцодиорити; кръстчета – гранодиорити; ромбчета – дайки. Трендове: I – шошонитов, II – високо-К калциево-алкален

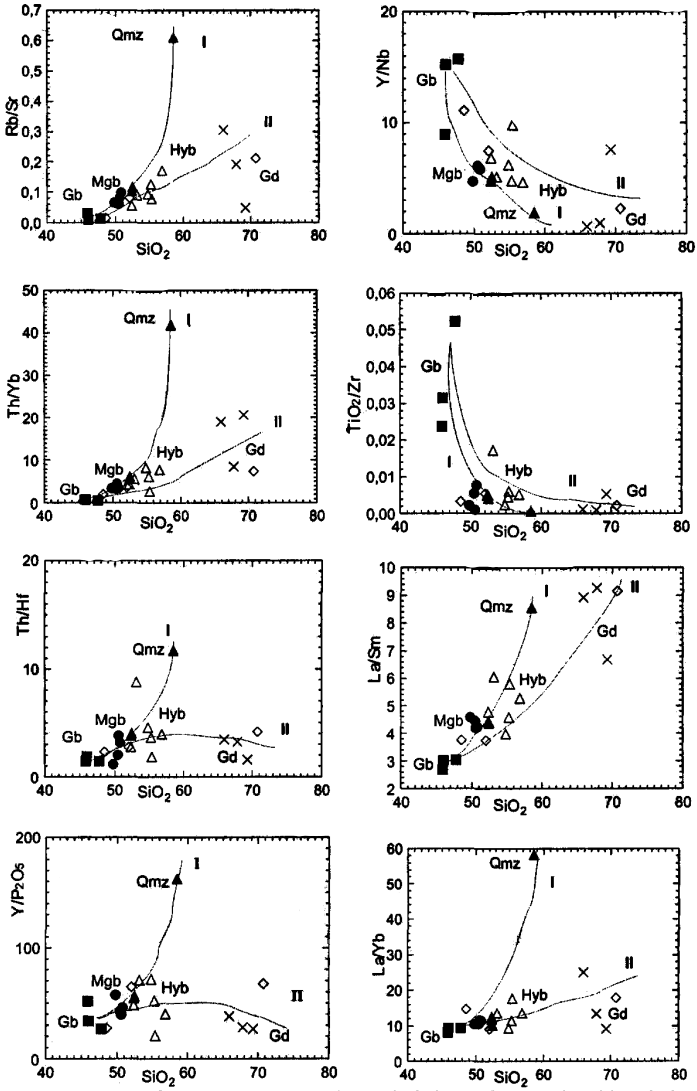

Fig. 7. Some noteworthy ratios for rocks of the Capitan-Dimitrievo pluton. The abbreviations, symbols and trends are the same in Fig. 5

Фиг. 7. Някои значими отношения за скали от Капитан-Димитриевския плутон. Съкращенията, символите и трендовете са същите както на фиг. 5

remarkable). This component somehow later on was mixed with the more primitive new basic input into the chamber. It is clear that the mafic component was derived from a mantle source not bearing plagioclases. Another alternative is the extreme composition of the quartz-monzonite to be result of the melt from the lower crust level, unusually reach in alkalies. Then the Eu-anomaly could reflect the plagioclase-bearing source characteristics of

Table 7. *Representative analyses of rocks (major oxides in wt. % and trace elements in ppm)*
Таблица 7. *Представителни анализи на скали (главни оксиди в тегл. % и елементи-следи в ppm)*

№	69-b	71-a	31-I	70-a	29	128	122	121	82-b	70-b
Rock	Xen	MGb	MGb	QMd	QMd	QMz	Gd	Gd	Gb-p	Gr-p
SiO_2	46.07	47.82	50.51	54.82	56.91	58.48	65.93	67.83	48.64	70.70
TiO_2	0.76	1.14	1.14	0.73	0.84	0.64	0.67	0.39	0.22	0.24
Al_2O_3	19.92	18.43	16.95	15.81	14.63	20.37	15.80	15.99	18.20	13.29
Fe_2O_3	5.80	4.50	4.97	5.17	5.05	3.38	1.03	1.29	6.30	1.61
FeO	4.73	6.04	5.53	4.49	4.08	0.60	2.45	1.01	5.07	2.45
MnO	0.34	0.37	0.39	0.36	0.25	0.05	0.07	0.05	0.35	0.33
MgO	3.26	5.00	4.43	4.00	3.53	1.34	1.12	0.82	3.68	1.18
CaO	11.12	10.50	9.16	7.81	6.91	6.98	3.87	3.87	10.20	3.19
Na_2O	3.29	3.50	3.33	3.32	3.14	3.91	4.29	4.21	3.80	3.16
K_2O	0.72	1.16	2.55	2.63	2.67	3.73	3.02	3.04	1.22	3.17
P_2O_5	0.75	0.83	0.73	0.49	0.58	0.50	0.59	0.72	0.91	0.17
H2O-	0.54	0.17	0.12	0.10	0.23	0.17	0.22	0.04	0.14	0.11
LOI	2.41	1.00	0.63	0.53	0.81	0.28	0.74	0.52	0.92	0.33
Total	99.71	100.46	100.44	100.26	99.63	100.43	99.80	99.79	99.65	99.93
Q	0	0	0	5.8	11.7	6.8	20.2	24.1	0	31.1
M	28.2	33.6	32.8	30.0	27.2	11.9	10.0	5.2	30.7	10.5
An %	57.4	52.7	45.7	42.1	40.3	44.9	29.1	29.6	47.4	32.2
Ba	269.5	341.4	468.4	404	414.4	2245.4	639.3	672.3	512.4	570.9
Rb	16.4	18.7	56.0	73.55	119	558.3	146.7	107.7	25.3	76.8
Sr	1737	1328	941	785.6	684.8	912.5	479.9	554.8	1672	359
Cs	1.09	2.94	1.77	2.4	5.06	12.47	7.24	2.85	2.47	0.82
Ta	0.81	0.19	0.44	0.69	0.26	3.72	2.23	1.59	0.18	0.53
Nb	1.69	1.48	5.14	5.65	5.04	42.36	33.76	20.93	2.29	5.08
Hf	0.85	0.93	5.265	7.24	4.55	24.69	15.29	11.27	2.04	2.49
Zr	24.1	21.8	204.2	292.7	159.9	843.6	559.2	444.3	66.1	106.5
Y	25.8	22.8	31.4	35.1	23.6	81.4	22.7	20.7	25.6	11.6
Th	1.68	1.43	10.94	33.01	18.28	289.6	53.53	37.00	4.91	10.49
U	1.13	0.52	3.61	7.60	5.97	17.59	21.43	6.07	1.76	2.44
Cr	24.17	30.0	42.5	30.5	23.6	1477.6	1242.1	376.9	20.98	56.1
Ni	4.76	6.28	8.14	7.22	4.04	58.45	60.71	22.33	1.60	27.52
Co	24.33	31.29	25.59	24.52	22.66	8.47	6.05	3.89	24.91	7.07
Sc	14.09	23.83	23.36	20.32	19.7	10.22	7.41	7.84	15.54	6.13
Cu	144.4	79.8	146	87.9	57.8	31.27	17.95	12.1	355.1	32.03
Pb	14.79	8.94	23.09	22.11	26.89	138.8	48.3	44.02	15.3	8.61
Zn	92.6	91.76	95.94	89.1	86.36	63.6	46.12	37.82	86.39	25.43
W	0.48	0.4	0.98	0.723	0.825	-	-	-	0.45	0.72
Mo	0.56	1.59	3.73	2.78	1.71	58.59	50.02	14.60	1.2	7.14
V	-	-	-	-	-	150.7	91.35	54.98	-	-
Ga	-	-	-	-	-	21.02	19.97	17.96	-	-
La	22.35	20.74	36.14	36.94	32.20	42.01	70.47	59.26	35.31	25.39
Ce	51.64	45.05	72.76	77.66	61.45	77.40	119.95	104.20	73.51	40.84
Pr	6.75	6.16	8.99	9.6	6.83	8.81	12.63	10.03	9.39	4.24
Nd	35.78	28.71	38.69	44.12	28.98	38.27	45.81	40.08	43.35	15.71
Sm	7.33	6.76	8.11	9.19	6.06	6.94	7.88	6.39	9.33	2.77
Eu	2.22	2.23	2.31	2.24	1.81	2.14	1.63	1.61	2.96	0.77
Gd	6.38	5.73	6.21	7.09	5.02	6.28	6.21	5.29	6.83	1.92
Tb	0.91	0.77	1.01	1.03	0.74	0.83	0.77	0.68	1.01	0.34
Dy	4.76	4.19	4.92	6.19	3.93	5.35	3.44	4.14	4.98	1.80
Ho	1.04	0.89	1.03	1.26	0.82	1.09	0.80	0.76	1.02	0.38

Table 7. Continued — Таблица 7. Продължение

Er	2.59	1.81	3.14	3.775	2.49	2.82	1.96	2.31	2.33	1.11
Tm	0.38	0.25	0.48	0.58	0.44	0.38	0.35	0.37	0.31	0.18
Yb	2.37	2.16	3.38	4.00	2.37	3.09	2.79	4.33	2.37	1.40
Lu	0.35	0.32	0.46	0.56	0.4	0.43	0.46	0.57	0.34	0.24

Notes: The analyses of the major oxides are wet silicate ones. Normative parameters: Q – quartz in %, M – mafic index (CIPW). Rock – modal nomenclature (MGb – monzogabbro, QMd – quartz-monzodiorite, QMz – quartz-monzonite, Gd – granodiorite, Gb-p – gabbro porphyry dyke, Gr-p – granite-porphyry, Xen – mafic xenolith)

Забележки: Главните оксиди са анализирани по класически мокър силикатен анализ. Нормативни параметри: Q - кварц в %, M – мафичен индекс (CIPW). Rock – модална номенклатура (MGb – монцогабро, QMd – квърцмонцодиорит, QMz - кварцмонцонит, Gd – гранодиорит, Gb-p – габропорфиритна дайка, Gr-p – гранит-порфирна дайка, Xen – мафичен ксенолит)

such rocks experienced melting under the influence of the hotter and mantle-derived magma emplaced to these levels. Again the mixing of the both end-components is plausible explanation.

Gabbro-monzodiorite-granodiorite mixing relationships are registered in the Fig. 8c, presenting the typical *REE*-patterns of the second mixing trend – high-K calc-alkaline one. The ratio $(La/Lu)_N$ 6.8-11.4 in the monzodiorite and quartz-monzodiorite samples. This range is not much unlike to the one of the monzogabbro, but it is a slightly lower than the one in the monzonite and much lower than the ratio in the quartz-monzonite. The same ratio is 11-16 in the granodiorite. The slope of the left side of the pattern is expressed in the ratio $(La/Sm)_N$ 2.3-3.7 in the monzodiorite and quartz-monzodiorite and 5.7-5.5 in the granodiorite. All mixing products of the end gabbro and granodiorite compositions are displayed just between these end distributions. The same is valid for the *ΣREE*, which increases from the gabbro, through monzodiorite (153-205 ppm) to the granodiorite (240-275 ppm). In contrast to the published data by Boyadjiev (1986) we did not record Eu-anomalies.

Dykes manifest nearly the same *REE*-characteristics (Fig. 9d) as in the other plutonic rocks. The slope of the enriched *REE*-patterns is less steep in the quartz-monzodiorite porphyry dyke than in the quartz-monzonite, the ratio $(La/Lu)_N$ being 6.2. The *LREE*-half of the pattern is also less steep – $(La/Sm)_N$= 2.3. The depleted pattern for the granite-porphyry dyke is an interesting detail, bearing to its residuim character.

Chondrite-normalized *REE*-patterns (Fig. 8a-d) are in accord with an enriched mantle source. All of them are generally similar and resemble closely those of the typical island-arc rocks with fractionated light *REE*.

Trace elements plotted on MORB-normalized spidergrams (Fig. 9) are divided in the same manner as for the *REE*-patterns (different trends of gabbro, shoshonitic, high-K calc-alkaline and dyke rocks). The most noteworthy characteristic of the diagrams is the typical negative Ta and Nb anomalies found in the calc-alkaline arcs. All patterns are typical of arc magmas in being predominantly *LILE*-enriched and HFSE- and Cr and Sc depleted. Subduction-enriched mantle source is characteristic for the gabbro and its pattern differs from the one of the hybrid rocks with lower *LILE*-enrichment and deeper negative peaks at Ta, Nb, Zr and Hf. The hybrid monzogabbro representatives are closer in their MORB-patterns to the monzonites. Such difference is compatible to the idea that the monzonites and the monzogabbro are results of the mixing between the quartz-monzonite and the gabbro. The source of the gabbro end-member was more enriched in zircon, hornblende, and rutile accessories than the one of the quartz-monzonite. Typical of the gabbro is the positive peak for P in contrast to the

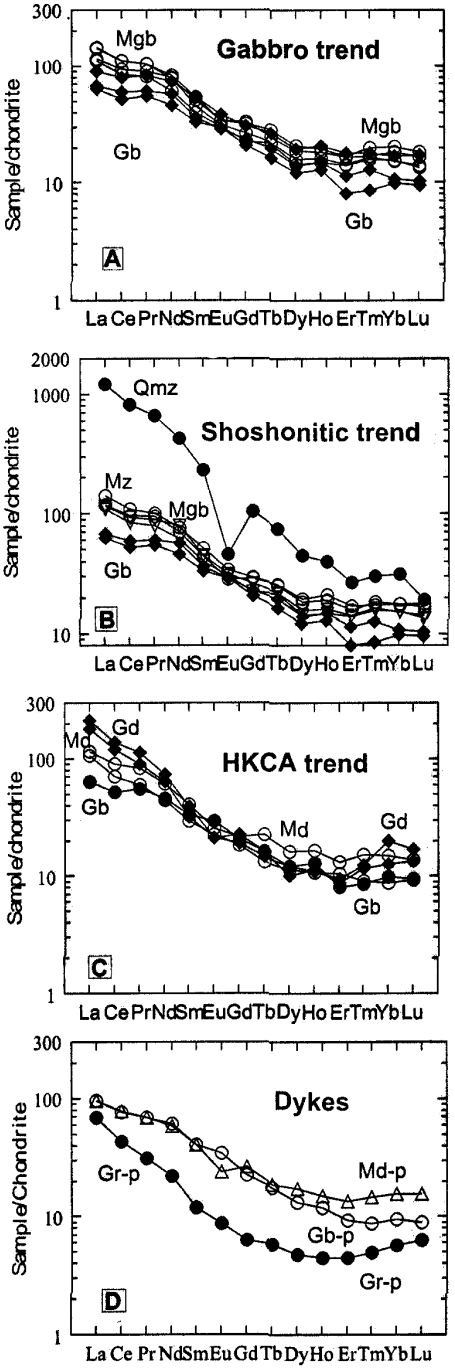

quartz-monzonite end-component. This peak disappears in the other rock varieties in the shoshonitic trend and in the quartz-monzonite sample a deep negative anomaly for P is recorded. Strong fractionation of P could be realized by fractionation of apatite. The second mixing line is evidenced clearly in Fig. 9c. The general outline of the patterns is more ore less similar. Monzodiorite hybrid varieties are emplaced between the both end-magma components (gabbro and granodiorite). The only essential difference of the granodiorite patterns from the ones of the other rock types is the behaviour of the Cr with its high positive anomaly. This feature is repeated in the granite-porphyry dykes (Fig. 9d). As the Cr is one important conservative element, this should be the result of the different magma sources of the both end-magmas of this mixing line. Melting of the lower crust from hornblende-rich source could produce the granodiorite, while the gabbro is likely to have mantle source, contained chromites in addition to pyroxene, olivine and biotite and hornblende. The granite-porphyry dykes bearing close similarity with the granodiorite are closer in their geochemical signature to this end-member of the mixing process.

Volcanic-arc setting is well substantiated in the discrimination diagram of Pearce et al. (1984) presented in Fig. 10.

Fig. 8. Selected chondrite-normalized *REE*-patterns for representative rock samples arranged in the following groups: a – gabbro-monzogabbro; b – gabbro-monzogabbro-monzonite - quartz-monzonite (shoshonitic trend); c – gabbro- monzodiorite and quartz-monzodiorite – granodiorite (high-K calc-alkaline trend); d – dykes

Фиг. 8. Избрани хондрит-нормализирани модели на *REE* за представителни скални проби подредени в следните групи: a – габро-монцогабро; b – габро-монцогабро-монцонит-кварц-монцонит (шошонитов тренд); c – габро-монцодиорит-кварц-монцодиорит -гранодиорит (високо-К калциево-алкален тренд); d - дайки

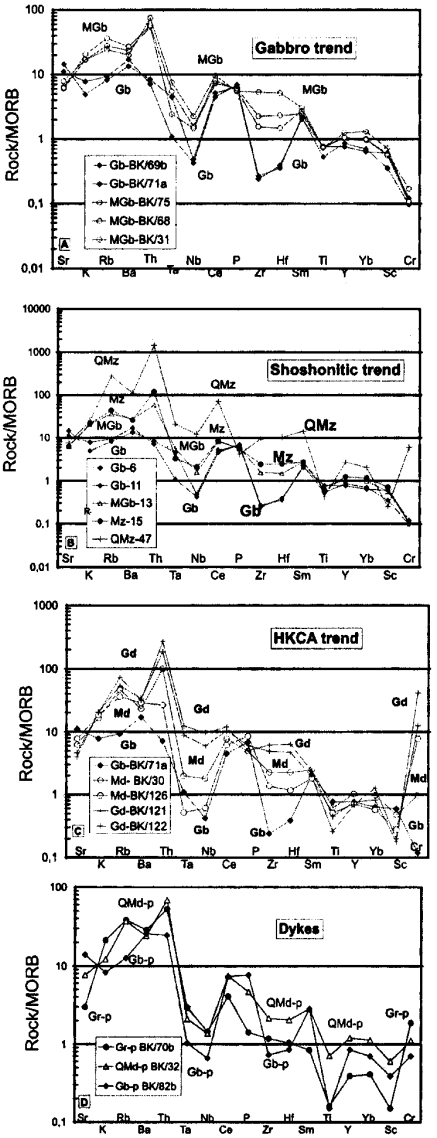

Fig. 9. Selected MORB-normalized trace-element patterns for representative rock samples arranged in the same way as in Fig. 8

Фиг. 9. Избрани MORB-нормализирани модели на разпределението на елементите-следи за представителни проби, подредени по същия начин както на фиг. 8

Geothermometry and geobarometry

The applied geothermometer of Blundy and Holland (1990) yielded reasonable magmatic temperatures of crystallization between 700 and 900°C (Table 8). The temperature estimations for the individual samples are harmonised with the pressure estimations using the geothermo-barometric method of Anderson and Smith (1995) on selected amphibole-plagioclase pairs in equilibrium. The revealed general negative correlation between the pressures and the temperatures of crystallization is a strange peculiarity not in line with the normal regularity derived from crystal fractionation of a common parental magma. The lack of thermal trend in time or in the seeming sequence of the rock varieties, arranged in their acidity, is also significant.

Pressure and thermal calculations cluster usually in two levels. A normal temperature

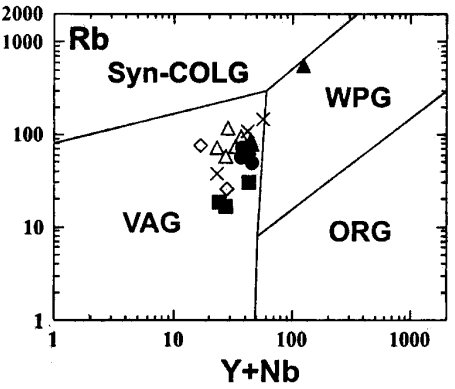

Fig. 10. Rb vs. (Y + Nb) discriminant diagram after Pearce et al. (1984). Syn-COLG – syn-collisional granites; WPG – within-plate granites; VAG – volcanic-arc granites; ORG – ocean-ridge granites. The sample symbols are the same as in the Fig. 6

Фиг. 10. Дискриминантна диаграма Rb vs. (Y + Nb) по Pearce et al. (1984). Syn-COLG – синколизионни гранити; WPG – вътрешно-плочови гранити; VAG – вулканско-дъгови гранити; ORG – океанско-хребетни гранити. Символите са същите както на фиг. 6

Table 8. *Averaged thermobarometric estimations from amphibole-plagioclase pairs in rocks from Capitan-Dimitrievo pluton*
Таблица 8. *Усреднени термобарометрични оценки от амфибол-плагиоклазови двойки от скали на Капитан-Димитриевския плутон*

Rocks	*T*°C	*P* kbar	Depth in km.
Gabbro	c- 835-900	3.7-3.9	10.0-11.0
	r- 770-850	2.3-2.5	6.0-7.0
Monzogabbro	c- 850-870	1.8-1.9	5.0-5.5
	r- 800-840	2.4-3.0	7.0-8.0
Monzodiorite	c-900-970	2.2-2.3	6.0-6.5
	r- 870-900	2.2-2.3	6.0-6.5
Quartz-monzodiorite	c-820-850	5.9	16.0
	r- 700-900	1.1	3.0
Granodiorite	c- 750-770	3.8-4.8	10.0-13.0
	r- 735-745	3.2-4.0	8.0-10.0
	r- 720-730	2	5.0-6.0

Notes: *P* is estimated after Anderson and Smith (1995) and *T* is after Blundy and Holland (1990). c-cores; r – rims. The averaged results are based on 25 mineral pairs
Забележки: Наляганията са оценени по Anderson, Smith (1995), а температурите – по Blundy, Holland (1990). с – ядра; r – периферия на минерални зърна. Усреднените резултати са от 25 равновесни минерални двойки

zoning between the cores and the rims is established only for the gabbro pairs. The reverse temperature zonings are more typical for the hybrid rock varieties. The irregular distributions of the pressure and temperature estimations are probably due to magma-mixing evolution. Reverse temperature changes could be traces of such processes. We conclude, therefore, that the Capitan-Dimitrievo magmatic system was open and actively mixing periodically with more primitive magmas. The heating of the mantle derived basic magma produced the crust-derived melting (granodiorite partial magma) at a level approximately of 8-12 km. The magmatic lower chamber of crystallization and differentiation was at level of about 16 km (some of the quartz-monzodiorites bear traces of this level in their amphibole-plagioclase pairs). The segregated granodiorite magma moved to the level of around 4-8 km as a crystal-rich mush. Later influx of more-primitive magma (gabbro in composition) started its crystallization at about 10 km (the first cluster of pressure estimates in the gabbro) and rises to the level of 4-8 km, where the mingling with the acid granodiorite mush was realized. This level is recorded in the monzogabbro, monzodiorite and other hybrid rock varieties by the unusual reverse zonings or the appearance of peaks of high anorthite compositions in the plagioclases. The system was in approximate thermal steady state in this level of mixing. The homogenization between the "drier" and hotter granodioritic mush and the richer in water more primitive gabbro magma happened probably at this level. It is difficult to gain insight into the dynamics of the complex processes of magma mixing, even with detailed eyewitness of the field relations and petrographic and mineralogical documentation. In spite of that, using the estimates of temperature, total pressure and water content of the magma reservoir, we could have at least an idea for the availability of such manifestations, like the presented new data in the case of Capitan-Dimitirevo pluton, bearing to the new idea of its origin.

Isotope geochronology and geochemistry

U-Pb dating on single zircons from the Q-monzodiorite variety of the pluton (Table 9) reveals an upper intercept intrusion age of 78.7 ± 1.8 Ma, using all data points (Fig. 12; the corresponding point of zircon 1 is not shown on the graphic). Some of the zircons have negligible lead inheritance (points 1 and 4 of Table 9) or lead loss (zircon 5), which leads to the bigger 2-σ error of the age determination. The mean $^{206}Pb/^{238}U$ age of the two most concordant points is calculated as 78.54 ± 0.13 Ma and interpreted therefore as the time of the crystallization of the Q-monzodiorites.

The ε–Hf values - corrected for the time of formation (T 79 Ma) of all measured zircons change in a narrow range from +8.10 to +9.20

Table 9. *U-Pb zircon isotope data for the quartz-monzodiorite sample AvQ-015*
Таблица 9. *U-Pb изотопни данни върху циркони от кварцмонцодиоритовия образец AvQ-015*

N	Size fraction, μm	weight in mg	#	U ppm	Pb ppm	$^{206}Pb/^{204}Pb$	$^{206}Pb/^{238}U$	2σ error %	$^{207}Pb/^{235}U$	2σ error %	$^{207}Pb/^{206}Pb$	2σ error %	$^{206}Pb/^{238}U$ apparent ages	$^{207}Pb/^{235}U$ apparent ages	$^{207}Pb/^{206}Pb$ apparent ages	Rho
1	-250+200	0.2387	prism pile beige	109.22	2.24	128.27	0.012357	2.09	0.082340	7.46	0.048327	6.76	79.17	80.34	115.33	0.46
2	-250+200	0.1136	prism pile beige	137.16	1.96	701.29	0.012245	1.03	0.080360	1.14	0.047597	0.47	78.46	78.48	79.28	0.91
3	-250+200	0.1222	prism pile beige	146.81	2.12	494.38	0.012014	1.44	0.079092	1.82	0.047747	1.06	76.99	77.29	86.73	0.81
4	-250+200	0.0893	prism abr	109.84	2.13	147.4	0.012419	0.58	0.081911	1.62	0.047838	1.44	79.56	79.94	91.25	0.48
5	-125+63	0.2708	prism abr	129.11	1.76	1070.8	0.012277	0.60	0.080511	0.68	0.047561	0.31	78.66	78.62	77.48	0.89

#abr - abraded, prism – prismatic; Rho - correlation coefficient $^{206}Pb/U - ^{207}Pb/^{235}U$
#abr – абрадиран, prism – призматичен; Rho – корелационен коефициент $^{206}Pb/^{238}U - ^{207}Pb/^{235}U$

Table 10. *Hf isotope data for zircons of Q-monzodiorite AvQ-015*
Таблица 10. *Hf изотопни данни за циркони от кварцмонцодиорит (образец AvQ-015)*

No	$^{176}Hf/^{177}Hf$	2σ error	ε-Hf	ε-Hf $T_{79\,Ma}$
1	0.282966	0.000002	6.86	8.10
2	0.282977	0.000003	7.25	8.49
3	0.282984	0.000002	7.50	8.74
4	0.282981	0.000002	7.39	8.63
5	0.282997	0.000003	7.96	9.20

Numbers as in Table 9
Номерата са същите както на таблица 9

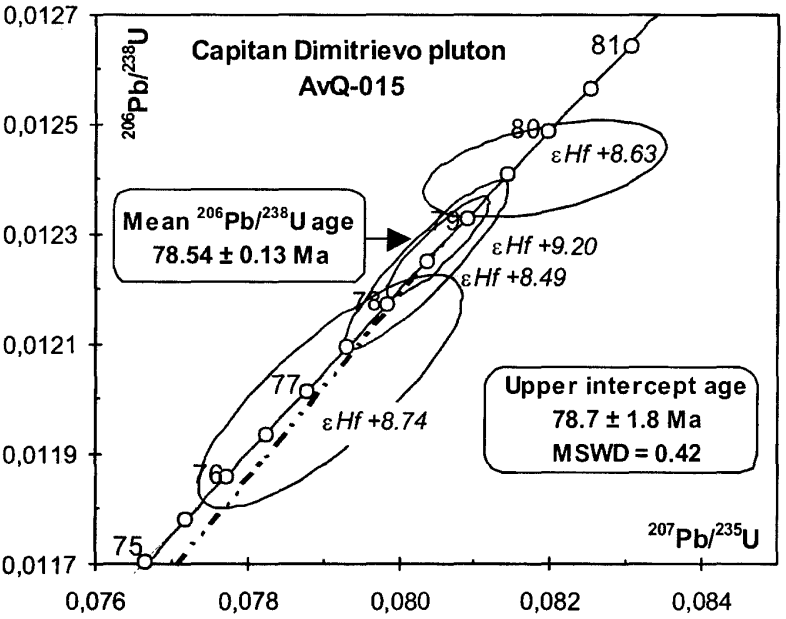

Fig. 11. U-Pb concordia diagram of zircons from monzogabbro sample AvQ-0015. The mean age is calculated from the weighted average of the $^{206}Pb/^{238}U$ ratio

Фиг. 11. U-Pb диаграма конкордиа на циркони от монцогаброва проба AvQ-0015. Средната възраст е изчислена от претегленото средно на отношението $^{206}Pb/^{238}U$ ratio

(Table 10) indicating an island arc basalt mantle dominated magma source (Nowell et al., 1998), contaminated negligible with continental crust material. This conclusion is in accordance with the major chemistry of sample BK/32, determined as one of the basic members of Capitan-Dimitrievo pluton. The zircon population of the rock consists of similar beige short prismatic zircons without older cores or lead inheritance and they are typical for gabbro magma without crustal contamination.

Sr and Nd isotope characteristics give evidence for both processes: fractionation of normal MORB or enriched mantle magma and mixing with at least one type (but probably two types) of crustal dominated member. Two distinctive trends are shown in Figs. 12a-c, 13 and 14. Fig. 12a, using $(^{87}Sr/^{86}Sr)_i$ versus SiO_2 content: in the first group (samples 69a, 71a, 31-I, 118 and 128) the initial strontium ratio remains constant with the increase of SiO_2. A simple fractionation of enriched mantle derivative magma for this group with the deepest initial Sr could be supposed. An alternative explanation could be the mixing between the already evolved by fractionation quartz-monzonite member and more primitive basic magma influx, derived from the same enriched mantle source. For the second group of samples (70a, 29, 121, 122 and 70b) the increase of the $(^{87}Sr/^{86}Sr)_i$ of rock varieties is in line with this of SiO_2. The same relations are observed on the 1/Sr*100 vs. $(^{87}Sr/^{86}Sr)_i$ diagram (Fig. 12b), where the increasing of the $^{87}Sr/^{86}Sr$ ratios is correlated with a decreasing of the Sr content. We consider this group therefore as a result of mixing with radiogenic crustal material. The observed correlations are in accordance with the availability of the second geochemical trend between granodiorites and the gabbro.

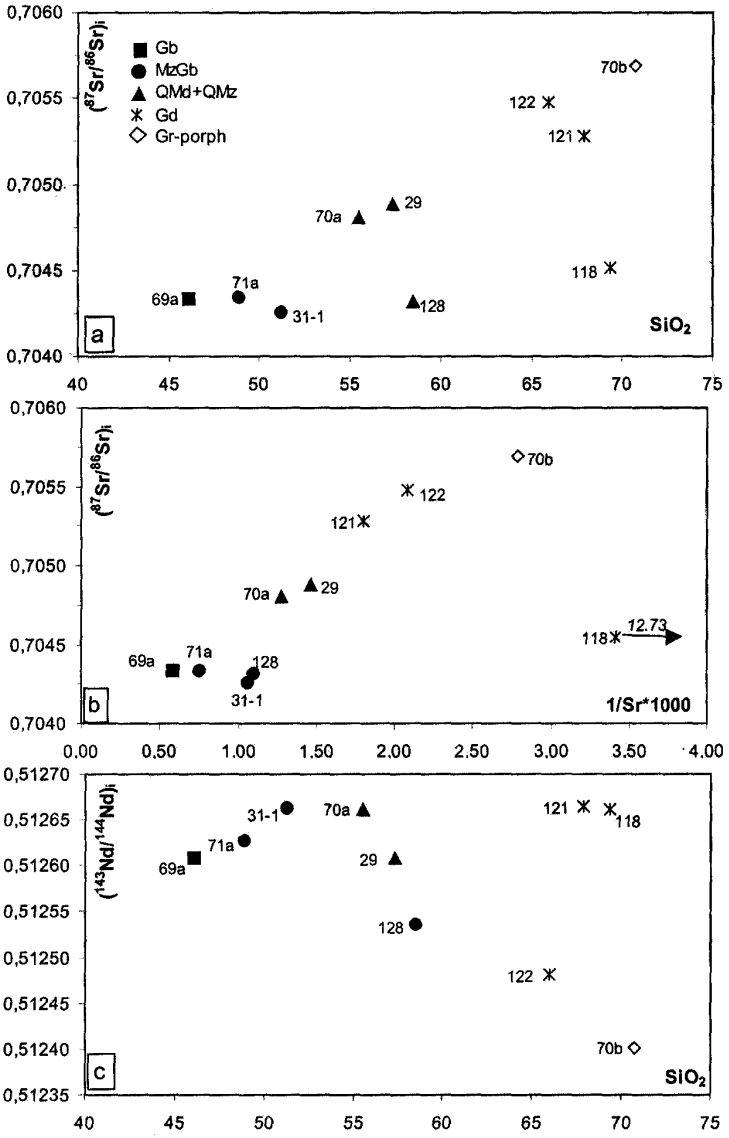

Fig. 12a. SiO_2 vs. $(^{87}Sr/^{86}Sr)_I$, b. 1/Sr)*1000 vs. $(^{87}Sr/^{86}Sr)_I$ and c. SiO_2 vs. $(^{143}Nd/^{144}Nd)_I$ diagrams for samples of the Capitan-Dimitrievo pluton demonstrating the influence of the assimilation and mixing on the characteristics of the intermediate and acid rock varieties

Фиг. 12a. SiO_2 vs. $(^{87}Sr/^{86}Sr)_I$, b. 1/Sr)*1000 vs. $(^{87}Sr/^{86}Sr)_I$ и c. SiO_2 vs. $(^{143}Nd/^{144}Nd)_I$ диаграми за проби от Капитан-Димитриевския плутон, показващи влиянието на асимилацията и смесването върху характеристиките на промеждутъчните и кисели скални разновидности

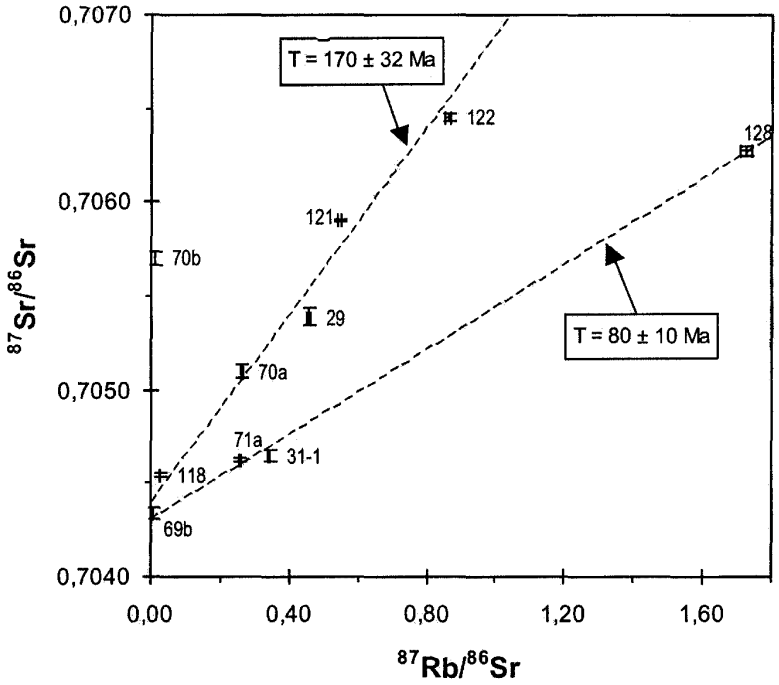

Fig. 13. Rb-Sr isotope diagram for rock samples of the Capitan-Dimitrievo pluton. The two reference lines correspond to ages of 80 ±10 Ma (MSWD=11) and 170 ± 32 Ma (MSWD=88). Comments – in the text

Фиг. 13. Изотопна диаграма Rb-Sr за проби от Капитан-Димитриевския плутон. Двете линии съответстват на възрасти от 80 ±10 Ma (MSWD=11) и 170 ± 32 Ma (MSWD=88). Коментарии – в текста

Speculatively we tried to calculate the age of the two groups of samples, as they are present also on the Rb-Sr isotope diagram (Fig. 13). The slope of the reference line corresponds to an age of T 80 ± 10 Ma for this group. The obtained age is in good agreement with the real age of the magmatic activity, as it is determined using the U-Pb zircon method (Fig. 11). The second group plots on a reference line, corresponding to an age of T 170 ± 32 Ma, which has no geological meaning. This line is a result of mixing of the mantle dominated Cretaceous magma with older crustal (radiogenic isotopes rich) materials.

On the SiO_2 vs.$(^{143}Nd/^{144}Nd)_i$ diagram (Fig. 12c) the two trends are observed again: first, with simultaneous increase of SiO_2 and decrease of the neodimium ratio, and the one of quite constant $(^{143}Nd/^{144}Nd)_i$. Some of the rock samples deviate from the usual inverse negative correlation of $(^{87}Sr/^{86}Sr)_i$ and $(^{143}Nd/^{144}Nd)_i$ (Tabl. 11, Fig. 14). One possible expla-nation is the more mobile behaviour of Sr compared to Nd and hence the increase of the initial Sr ratio, when the Nd ratio changes just negligible (the horizontal trend on Fig. 14). In this case the vertical trend on Fig. 14 (rock varieties, which we interpreted as a result of fraction crystallization of initial mantle magma) is due on an initial Nd-inhomogeneity of the mantle source. Such trend could be only explained with mantle enrichment, despite the points are lying to the left of the out pointed enriched mantle (EM1 field of Zindler and Hart (1986). The decreasing Nd ratios of sample 70b

Table 11. *Rb-Sr and Sm-Nd isotope data for whole rock samples of the Capitan-Dimitrievo pluton*
Таблица 11. *Rb-Sr и Sm-Nd изотопни данни за скални общи проби от Капитан-Димитриевския плутон*

Nr	Rock type	Rb (ppm)	Sr (ppm)	$^{87}Rb/^{86}Sr$	2σ error	$^{87}Sr/^{86}Sr$	2σ error	$(^{87}Sr/^{86}Sr)_{i80}$	Sm (ppm)	Nd (ppm)	$^{147}Nd/^{144}Nd$	2σ error	$^{143}Nd/^{144}Nd$	2σ error	$^{143}Nd/^{144}Nd$ T=80	ε-Nd T=80
71a	MGb	150.2	1686.2	0.2576	0.0026	0.70463	0.00001	0.70434	8.17	38.5	0.1280	0.0013	0.512627	0.000007	0.512560	0.49
31-I	MGb	128.5	1084.1	0.3429	0.0034	0.70464	0.00003	0.70426	8.11	38.7	0.1320	0.0013	0.512627	0.000008	0.512594	1.13
29	QMd	96.38	611.9	0.4556	0.0046	0.70539	0.00005	0.70488	6.07	29.0	0.1263	0.0013	0.512609	0.000007	0.512543	0.15
70a	QMd	73.55	785.5	0.2643	0.0026	0.70510	0.00004	0.70480	9.19	44.1	0.1312	0.0013	0.512661	0.000006	0.512592	1.18
69b	Gb	16.42	1737.0	0.0033	0.0000	0.70434	0.00003	0.70433	7.33	35.8	0.1236	0.0012	0.512609	0.000011	0.512544	0.18
70b	Gr-p	30.01	970.1	0.0109	0.0001	0.70570	0.00004	0.70569	2.77	15.7	0.1064	0.0011	0.512402	0.000018	0.512346	-3.68
118	Gd	6.61	78.57	0.0293	0.0003	0.70455	0.00001	0.70451	0.30	1.47	0.1235	0.0012	0.512662	0.000025	0.512597	1.22
121	Gd	107.7	554.7	0.5480	0.0055	0.70591	0.00001	0.70528	6.39	40.1	0.0961	0.0010	0.512665	0.000006	0.512615	1.55
128	QMz	558.3	912.5	17.260	0.0173	0.70628	0.00002	0.70431	4.68	27.0	0.1046	0.0010	0.512537	0.000011	0.512482	-1.03
122	Gd	146.7	479.9	0.8628	0.0086	0.70646	0.00002	0.70547	7.88	45.8	0.1034	0.0010	0.512481	0.000011	0.512427	-2.11

Abbreviations as in Table 7
Съкращенията са както в таблица 7

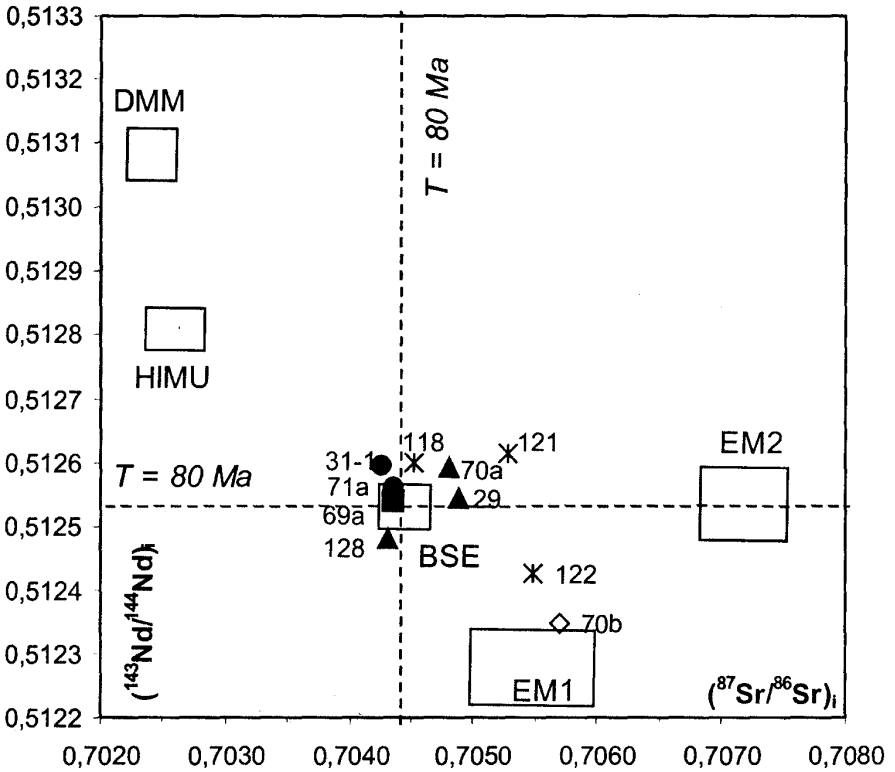

Fig. 14. $(^{87}Sr/^{86}Sr)_I$ vs. $(^{143}Nd/^{144}Nd)_I$ diagram for rock samples of the Capitan-Dimitrievo pluton. Fields of the DMM (depleted MORB mantle), HIMU (magma source having a high μ – $^{138}U/^{204}Pb$ ratio), EM1 and EM2 (enriched mantle 1 and 2) and BSE (bulk silicate earth) are given (corrected for 80 Ma) according to Zindler and Hart (1986). Dashed lines correspond to the Sr and Nd isotope values of the undifferentiated reservoir – identical to CHUR (DePaolo, 1988; Faure, 2001), corrected for 80 Ma

Фиг. 14. Диаграма $(^{87}Sr/^{86}Sr)_I$ vs. $(^{143}Nd/^{144}Nd)_I$ за скални проби от Капитан-Димитриевския плутон. Полетата за DMM (обеднена MORB мантия), HIMU (магмен източник с високо отношение μ – $^{138}U/^{204}Pb$), EM1 and EM2 (обогатена мантия 1 and 2) and BSE (обобщено за силикатния земен слой) са дадени (коригирани за 80 Ma) по Zindler и Hart (1986)

and 122 show the participation of a second source material during the fractionation process, probably a type of EM1 source (Fig. 14).

Discussion of the results

The Capitan-Dimitrievo pluton marks the youngest magmatic activity in the Central Srednogorie (von Quadt et al., 2003) and shows similar isotope-geochemical characteristics with the composite plutons in the southern parts of this zone (Kamenov et al., 2003). The magmatic system has been an open system with a periodic influx of primitive magma. We found support for this in the field observations, mineral chemistry fluctuations and in the revealed two geochemical trends. The isotope data also reveal pseudo-isochrones

and two mixing lines. We may figure interplay of three end-components responsible for the rock variety within the pluton. The passage of large masses of subduction-related magma through the crust may transfer heat and perhaps volatiles to the crust to cause melting if sufficient basalt volume traverses the crust (Marsh, 1984). It is quite possible that mafic melts and their dissolved volatiles may interact more directly with granitic melts once silicic magmas begin to accumulate within the crust. Because the mafic magma has a higher crystallization temperature, it will also tend to partially quench against the cooler acid mush and would underplate the less dense silicic magma. The last one will act as a density and thermal barrier for upwelling mafic magma.

The original mantle source undoubtedly was metasomatized to some extent (hornblende- and biotite-bearing), based on the enriched trace-element patterns, found in most mafic samples of the pluton. The Sr and Nd isotope data provide support for such an enriched mantle source typical for an island arc environment – in contrast to the Hf data showing the domination of the mantle matter. Probably, the Hf data detect the characteristics of the more primitive basic input of magma, which have come from deeper MORB-like source, while the Sr-Nd data were typical for the magma evolution in the lower chamber of differentiation, located somehow in the more moderate level (let us say around 15 km, according to our geobarometric estimations). The last chamber was the place where an essential part of the bulk magma evolution occurred, probably. At this level, the subduction-related magma through differentiation evolved from gabbro to rich in K quartz-monzonite. The melted lower crust source either was built up by amphibolites or metadiorites to produce granodiorite melt. The crust-derived granodioritic system crystallized at level of about 10 km underplated by the crystallizing gabbro. The level of 4-8 km appears to be the last stop of the magma interactions. At this level the two lines of mixing were realized. The first one was between the rich in potassium quartz-monzonitic fractionation-produced partial magma from one side (the first mixing component) with the influx of parental more primitive magma (the second mixing component) raised some later on from the same 15 km chamber level. The second line was between granodioritic crust-derived magma (the third mixing component) with basic influxes of mantle-derived mafic and more primitive magma (the second mixing component). Convection and mixing in the granitic magma transported thermal energy throughout the body, aiding an additional assimilation, and at times disrupting the mixed, semi-solid boundary layer, strewing fragments of the mixed zone throughout the magma chamber. Granitoid plutons formed by such a mixing process can be quite variable in composition because their characteristics depend on the nature of granitic melts formed in the crust, the composition of more mafic magmas, which interact with them, the relative quantity of such mafic magmas, and the degree of interaction (Whitney, 1988). This was just the case in Capitan-Dimitrievo pluton, where not only the rock variety is great, but the mixing portions of the mafic component were higher than the acid ones.

No economic ores are known to exist related to the pluton, in spite of its resemblance to the other ore-productive plutons in the zone. Poor iron-copper vein-type and disseminated type mineralizations occur within the plutonic rocks, some of them prospected by trenches and even drilling, but they turned out to be only of academic significance. The rapid uplift and the deeper erosion than in the other ore-magmatic centers in the zone are probably one of the reasons for its barren character at the today's surface. The lack of intensive alterations of the rocks confirms such a speculation. We did not find even a sub-solidus fluid reworking of the rock-forming amphiboles, which usually are very sensitive to low-temperature equilibration. The interacting magmas carried enough water and fluids to produce hydrothermal economical concentrations of sulphide ores and it is most likely that such ores existed outside of the now a

day's surface of the pluton. Neither temperature, nor the pressure estimates of the magma crystallization are too much different from the crystallization conditions deduced out of the other plutons in the Srednogorie zone. The oxidizing conditions were also similar. The more primitive character of the mantle-derived component of magma mixing and the lower degree of melting of its metasomatized mantle source (Kamenov et al., 2003) is a subtle difference with the other magmatic centres in the zone. The involvement of crust-derived melts from the Rhodopian metamorphic units, combined with interrelations with island-arc differentiated ones and with more primitive magmas explains the observed geochemical and isotope peculiarities of the rocks, but hardly has direct influence on its barren nature. It is possible the input of anatectic melt from the Rhodopian tectonic units, instead of the Srednogorie unit, to have some effect on the case, but with the available geochemical and isotope data, the comparison between the both crustal materials is not possible.

Conclusions

1. The petrographic diversity in the Capitan-Dimitrievo pluton is a result of magma-mixing process, combined with fractional crystallization. The complex interplay between three components (gabbro, granodiorite and quartz-monzonzonite magmas) is responsible for the petrological features of the rocks.
2. The chemical range within the rocks of the pluton confirms the presence of two serial trends – a high-K calcalkaline and a shoshonitic, the last one prevailing.
3. Tectonic discriminations support the subduction-related arc-like affinity of the plutonic rocks. An enriched and metasomatised hornblende- and biotite-bearing mantle source was involved in the derivation of the parental melt basic component of mixing.
4. Compositional variations in the rock-forming minerals found arguments for the physical and chemical conditions of crystallization and the levels of mixing and fractionation. The prevailing temperatures of crystallization were moderately high and the last level of crystallization and mixing with the granodiorite crust-derived magma was 4-8 km.
5. The Capitan-Dimitrievo pluton should be affiliated to the same metallogenic province of the Srednogorie zone. The petrological correlation of the pluton with the other ore-productive centers in the zone is an argument for its ore-productive potential, in spite of the fact that at today's erosion level the prospects for finding economic ores are not promising. The rich mineralized part of the island-arc system probably was destroyed within several million years after the uplift of the arc area.
6. The new isotope data reported here provide the first persuasive evidence for its Late Cretaceous age – 78.5 Ma. Isotope ratios and trace-element data confirm that the pluton had crystallized out of the most uncontaminated magma, compared with the other magmatites of the zone.

Acknowledgements: This research has been carried out in the framework of the GEODE programme of the European Science Foundation and is supported by the Swiss National Science Foundation through the SCOPES Joint Research Projects 7BUPJ62396. We appreciate the help of Jivko Ivanov and Dimo Dimov in part of the fieldwork. Our thanks are due to E. Landjeva performed the new wet silicate analyses and to Christo Stanchev for assisting in microprobe analyses. We acknowledge also the help of Evgeniya Genova for drawing of some of the figures.

References

Abdel-Rahman, A-F.M. 1994. Nature of biotites from alkaline, calc-alkaline and peraluminous magmas. *J. Petrol.*, **35**, 525-529.

Anderson, J.L., D.R. Smith. 1995. The effects of temperature and fO_2 on the Al-in-hornblende barometer. *Amer. Mineral.*, **80**, 549-559.

Andrew, C. 1997. The geology and genesis of the Chelopech Au-Cu deposit, Bulgaria: Europe's largest gold resource. In: *Europe's Major Gold Deposits*, Abstracts volume, Newcastle, Northern Ireland, Irish Association for Economic Geology, 68-72.

Bogatikov, O.A., N.P. Michailov, V.I. Gonshakova (eds). 1981. Classification and Nomenclature of

Magmatic Rocks. Moscow, Nedra, 160 p. (in Russsian).

Blundy, J. B., T. J. B. Holland. 1990. Calcic amphibole equilibria and a new amphibole-plagioclase geothermometer. *Contrib. Mineral. Petrol.*, **104**, 208-224.

Bonchev, G. 1938. The rock composition and geological structure of the basin of the river Krichim with a view of water use for practical and economic aims. *Rev. Bulg. Acad. Sci., Natural and Mathematical Sciences*, **57**, 55-75 (in Bulgarian).

Boyadjiev, S. 1986. Petrology and geochemistry of Capitan-Dimitrievo pluton. *Geochem. Mineral. Petrol.*, **20/21**, 97-127 (in Bulgarian with English abstract).

Boyadjiev, S., P. Lilov, 1981. Potassium-argon determinations of the Alpine intrusions from the Central Srednogorie. *C. R. Bulg. Acad. Sci.*, **34**, 4, 549-551.

Boyadjiev, S., V. Ivanova-Panayotova. 1982. Contact manifestations in the southeastern flank of Capitan Dimitrievo pluton. *Geochem. Mineral. Petrol.*, **16**, 68-76 (in Bulgarian with English abstract).

Dabovski, C. 1969. Structure of the Capitan Dimitrievo pluton. *Rev. Bulg. Geol. Soc.*, **30**, 2, 142-154 (in Bulgarian with English abstract).

Dabovski, C., A. Harkovska., B. Kamenov, B. Mavrudchiev, G. Stanisheva-Vassileva, Y. Yanev. 1991. A geodynamic model of the Alpine magmatism in Bulgaria. *Geol. Balcanica*, **21**, 4, 3-15.

David, K., M. Frank, R. K. O'Nions, N. S. Belshaw, J. W. Arden. 2001. The Hf isotope composition of global sea water and the evolution of Hf isotopes in the deep Pacific Ocean from Fe-Mn crusts. *Chem. Geol.*, **178**, 23-42.

De Paolo, D. J. 1988. *Neodymium Isotope Geochemistry*. Berlin, Springer, 316 p.

Dimitrov, S. 1939. Achievements and tasks of the petrographic studies in Bulgaria. *Ann. Univ. Sofia, Fac. Phys. Mathem.*, **35**, 3, Livre d' Hystoire Naturelle, 225-253 (in Bulgarian with abstract in German).

Dimitrov, S. 1946. The metamorphic and magmatic rocks in Bulgaria. In: *Fundamentals of the Bulgarian Geology. Ann. Direction Geol. and Mining Explor.*, part A, **4**, 61-93 (in Bulgarian).

Dobrev, T., M. Uzunova, N. Tashev. 1986. Structure of Maritsa deep fault zone and its expression in the geophysical fields. *Geol. Balcanica.*, **16**, 6, 33-59.

Faure, G. 2001. *Origin of Igneous Rocks: The Isotopic Evidence*. Berlin, Springer, 496 p.

Guenther, D., A. von Quadt, R. Wirz, H. Cousin, V. J. Dietrich. 2001. Elemental analyses using laser ablation-inductively coupled plasma-mass spectrometry (La-ICP-MS) of geological samples fused with $Li_2B_4O_7$; calibrated without matrix-matched standards. *Microchim. Acta*, **136**, 100-107.

Hibbard, M. J. 1981. The magma mixing origin of mantled plagioclases. *Contrib. Mineral. Petrol.*, **92**, 248-259.

Hibbard, M. J. 1991. Textural anatomy of twelve magma mixed granitoid systems. In: J. Didier, B. Barbarin, (eds.) *Enclaves and Granite Petrology*, Amsterdam, Elsevier, 431-444.

Kamenov, B. K., A. von Quadt, I. Peytcheva. 2003. New petrological, geochemical and isotopic data bearing on the genesis of Capitan-Dimitrievo pluton, Central Srednogorie, Bulgaria. In: *Geodynamics and Ore Deposit Evolution of the Alpine-Balkan-Carpathian-Dinaride Province.* Final GEODE-ABCD Workshop, Seggauberg, Austria. Programme and Abstracts, p. 31.

Kamenov, B. K., R. Moritz., R. Nedialkov, I. Peytcheva, A. von Quadt, S. Stoykov, Y. Yanev, A. Zartova. 2003. Petrology of Late-Cretaceous ore-magmatic centres from Central Srednogorie, Bulgaria: Magma evolution and paths. In: *Geodynamics and Ore Deposit Evolution of the Alpine-Balkan-Carpathian-Dinaride Province.* Final GEODE-ABCD Workshop, Seggauberg, Austria. Programme and Abstracts, p. 30.

Leake, B. E. et al. 1997. Nomenclature of amphiboles. Report of the Subcommittee on amphiboles in the IMA on new minerals and mineral names. *Eur. J. Mineral.*, **9**, 623-638.

Le Maitre, R. W. (ed.) 1989. *A Classification of Igneous Rocks and Glossary of Terms.* Oxford, Blackwell, 193 p.

Ludwig, K. R. 1988. PBDAT for MS-DOS; a computer program for IBM-PC compatibles for processing raw Pb-U-Th isotope data, version 1.00a. *US Geol. Survey,* Reston VA, 37 p.

Ludwig, K. R. 1991. ISOPLOT; a plotting and regression program for radiogenic-isotope data; version 2.53. *US Geol. Survey*, Reston VA, 39 p.

Morimoto, N. 1988. Nomenclature of pyroxenes. *Forschr. Miner.*, **66**, 2, 237-252.

Nowell, G. M., P. D. Kempton, S. R. Noble, J. G. Fitton, A. D. Saunders, J. J. Mahoney, R. N. Taylor. 1998. High precision Hf isotope measurements of MORB and OIB by thermal

ionization mass spectrometry: Insights into the depleted mantle. *Chem. Geol.*, **149**, 211-233.

Pearce, J., N. Harris, A. Tindle. 1984. Trace element discrimination diagrams for the tectonic interpretation of granitic rocks. *J. Petrol.*, **25**, 956-983.

Peccerillo, A., S. R. Taylor. 1976. Geochemistry of Eocene calc-alkaline volcanic rocks from the Kastamonu area, Northern Turkey. *Contrib. Mineral. Petrol.*, **58**, 63-81.

Richard, P., N. Shimizu, C. J. Allégre. 1976. $^{143}Nd/^{146}Nd$, a natural tracer: An application to oceanic basalts. *Earth Planet. Sci. Lett.*, **31**, 269-278.

Stacey, J. S, J. D. Kramers. 1975. Approximation of terrestrial lead isotope evolution by a two-stage model. *Earth Planet. Sci. Lett.*, **26**, 207-221.

Steiger, R. H, E. Jäger E. 1977. Subcommission on geochronology: Convention on the use of decay constants in geo- and cosmochronology. *Earth Planet. Sci. Lett.*, **36**, 359-362.

Thomas, W. M., W. G. Ernst. 1990. The aluminium content of hornblende in calc-alkaline granitic rocks: A mineralogic barometer calibrated experimentally to 12 kbars. In: R. J. Spencer, I. M. Chou (eds.) *Fluid-mineral interactions: A tribute to H. P. Eugster. Geochem. Soc. Spec. Publ.*, **2**, 59-63.

Tsuchiama, A. 1985. Dissolution kinetics of plagioclase in the melt of the system: diopside-anorthite-albite, and the origin of dusty plagioclase in andesites. *Contrib. Mineral. Petrol.*, **89**, 1-16.

von Quadt, A. 1997. U-Pb zircon and Sr-Nd-Pb whole rock investigations from the continental deep drilling (KTB). *Geolog. Rundschau*, **86**, 258-271.

von Quadt, A., I. Peytcheva, B. Kamenov, L. Fanger, C. A. Heinrich, M. Frank. 2002. The Elatsite porphyry copper deposit in the Panagyurishte ore district, Srednogorie zone, Bulgaria: U-Pb zircon geochronology and isotope-geochemical investigations of magmatism and ore genesis. In: D. J Blundell., F. Neubauer, A. von Quadt (eds.). *The Timing and Location of Major Ore Deposits in an Evolving Orogen. Geol Soc Spec Publ.*, **204**, London, 119-135.

von Quadt, A., I. Peytcheva, Ch. Heinrich, M. Frank, V. Cvetkovic, M. Banjesevic. 2003. Evolution of the Cretaceous magmatism in the Apuseni-Timok-Srednogorie metallogenic belt and implications for the geodynamic reconstructions: new insight from geochronology, geochemistry and isotope studies. In: *Geodynamics and Ore Deposit Evolution of the Alpine-Balkan-Carpathian-Dinaride Province.* Final GEODE-ABCD Workshop, Seggauberg, Austria. Programme and Abstracts, p. 60.

Whitney, J. A. 1988. The origin of granite: The role and source of water in the evolution of granitic magmas. *Geol. Soc. America*, **100**, 1886-1897.

Wones, D. R. 1981. Mafic silicates as an indicator of intensive parameters in granitic magmas. *Mineral. Mag.*, **31**, 191-212.

Yaranov, D. 1940. Geology of the northern slopes of Rhodopes Mountains between the towns Peshtera and Pazardjik, Plovdiv district, Bulgaria. *Rev. Bulg. Geol. Soc.* **12**, 2, 35-53 (in Bulgarian).

Zindler, A., S. R. Hart. 1986. Chemical geodynamics. *Ann. Rev. Earth Planet. Sci.*, **14**, 493-571.

Приета декември 2003 г.
Accepted December, 2003